

AN ABSTRACT OF THE THESIS OF

Michael E. Jacob for the degree of

Master of Science in Electrical and Computer Engineering

presented on May 28, 2009.

Title: Ultra Low Capacitance RFIC Probe

Abstract approved:

Leonard Forbes

In Radio Frequency Integrated Circuits (RFIC) or high frequency digital ICs, there is a demand to probe the internal nodes for testing. The ultra low capacitance RFIC probe presented in his work is a flexible tool for these applications. The probe utilizes the coupling between a tungsten needle and the inner conductor of a coaxial cable, forming a capacitor. The ultra low capacitance of the probe enables low probe loading on the circuit under test. With capacitive coupling, the probe output is the derivative of the input signal.

Through the use of probe calibration and Fourier transforms, the probed signal can be recovered. Probe calibration develops a transfer function enabling recovery of time domain signals. By utilizing a simple mechanical design, input impedance is maximized and parasitic components are minimized.

©Copyright by Michael E. Jacob

May 28, 2009

All Rights Reserved

Ultra Low Capacitance RFIC Probe

by
Michael E. Jacob

A THESIS

submitted to

Oregon State University

in partial fulfillment of
the requirements for the
degree of

Master of Science

Presented May 28, 2009
Commencement June 2009

Master of Science thesis of Michael E. Jacob presented on May 28, 2009.

APPROVED:

Major Professor, representing Electrical and Computer Engineering

Director of the School of Electrical Engineering and Computer Science

Dean of the Graduate School

I understand that my thesis will become part of the permanent collection of Oregon State University libraries. My signature below authorizes release of my thesis to any reader upon request.

Michael E. Jacob, Author

ACKNOWLEDGEMENTS

Academic

I would like to thank my major professor, Leonard Forbes, for his consistent guidance and encouragement on this work. His input made this work possible. Drake Miller provided a wide variety of help from reviewing publications to help with probe calibration and measurements. Also indispensable is Professor Andreas Weisshaar of the microwave group and his graduate students, Vikas Shilimkar, Steven Gaskill and Erik Vernon. Their lab equipment and advice facilitated testing of the probe. Brenton Gibson's CAD expertise transferred a design into a set of mechanical drawings. Ramin Zambaghi performed a peer review of this thesis. All of my Oregon State University EECS professors provided various aspects of knowledge enabling my research. Kartikeya Mayaram's RF class required learning Agilent ADS which was extensively used throughout this research. Special thanks go to Keith Riehl of Quater Research for research funding and construction of many probes for testing.

Personal

Much love to my partner, Martha Truninger for her love, support and encouragement for my entire 6 year academic adventure. Many thanks go to my parents, James & Virginia Cooper, and my sister, Kathleen Jacob. Their constant support has made academic life much more enjoyable.

TABLE OF CONTENTS

	<u>Page</u>
1 INTRODUCTION	2
1.1 Thesis Outline.....	5
2 PRIOR ART.....	6
2.1 Introduction	6
2.2 Comparisons of Probes.....	7
3 RFIC PROBE DESIGN.....	15
3.1 Introduction	15
3.2 Design Goal	15
3.3 Probe Tip Design.....	15
3.4 Capacitor Design	16
3.5 Preliminary Probe Calculations.....	18
3.6 Probe Modeling	20
3.7 RF Connector	23
4 RFIC PROBE CHARACTERIZATION	25
4.1 Introduction	25
4.2 S parameter Analysis.....	25
4.3 Transfer Function	27
5 HIGH FREQUENCY TEST CIRCUITS.....	31
5.1 Introduction	31
5.2 Colpitts Oscillator.....	31
5.3 Cross coupled oscillator	32
5.4 22nm Inverter	35
5.5 Summary	36
6 MEASUREMENTS AND SIGNAL RECOVERY	37
6.1 Introduction	37
6.2 Test Circuit Signal Recovery.....	37
6.3 Colpitts Oscillator.....	38
6.4 Cross Coupled Oscillator.....	40
6.5 22nm Inverter	42
6.6 Measured Pulse Generator Signal.	44
7 CONCLUSION.....	46
BIBLIOGRAPHY	47

LIST OF APPENDICES

Appendix	<u>Page</u>
A – Coaxial Specifications.....	51
B – Probe Design	53
C – Test Substrate	60
D – HSpice, 2D Circuit Simulation	61
E – Matlab, Probe Hand Calculations.....	66
F – Matlab, HSpice to FFT	68

LIST OF FIGURES

<u>Figure</u>		<u>Page</u>
1	Voltage vs. Time for a 1 GHz Input Signal and Ideal Probe Output.	4
2	Block Diagram of the Ultra Low Capacitance RFIC Probe.....	5
3	Circuit Diagram of 10X Voltage Probe.	7
4	Passive Oscilloscope Probe.	8
5	Active Oscilloscope Probe.	8
6	Active Oscilloscope Probe.	9
7	High Voltage Probe.	9
8	Active Shield Probe with Micro-Positioner [4].....	10
9	GSG Type RF Probe.....	11
10	High Impedance Probe.....	12
11	Photo of High Impedance Probe.	12
12	Capacitive Coupling.....	13
13	Laser Voltage Probe (LVP).....	14
14	Deriving the Capacitance Between Dissimilar Conductor Sizes.	17
15	Test Schematic to Optimize Needle Length and Coupling.....	18
16	Probe Input Impedance vs. Frequency.	19
17	EMDS Drawing of RFIC Probe.	21
18	Three Circuits Representing the RFIC Probe.....	22
19	Comparison of the Transfer Function.	23
20	Completed Probe Assembly.....	24
21	RFIC Probe Input and Output Signals.	25
22	VNA Setup for Probe Characterization.....	26
23	Analyzing the RFIC Probe on a Probe Station.....	26
24	Transfer Function Example.....	27
25	H1(s) Transfer Functions of EMDS and Actual RFIC Probes.....	29
26	Comparisons Between H1(s) and H2(s) Response.	29
27	Shifted H1(s) and H2(s) Comparison.....	30
28	5.8GHz Colpitts Oscillator.....	31
29	5.8GHz Cross Coupled Oscillator.....	34

LIST OF FIGURES (Continued)

<u>Figure</u>	<u>Page</u>
30	Inverter Modeled From 22nm CMOS Process..... 35
31	Colpitts Oscillator Output. 38
32	Probed and Un-probed Circuits are Compared. 39
33	Colpitts V1 Failure..... 39
34	Cross Coupled Oscillator Output. 41
35	Probed and Un-probed Circuits are Compared. 41
36	H1(s) Representation of 22nm Inverter Running at 10GHz. 43
37	H2(s) Representation of 22nm Inverter Running at 10GHz. 43
38	Output of the Second Inverter. 44
39	Sampled Probe Output 45
40	Pulse Generator Waveform and the Recovered Signal 45

LIST OF TABLES

<u>Table</u>		<u>Page</u>
1	Voltage Probe Variety	6
2	Node Impedances of Test Circuits.....	36
3	Colpitts Oscillator Spectral Analysis.....	40
4	Cross Coupled Oscillator Spectral Analysis.....	42

ULTRA LOW CAPACITANCE RFIC PROBE

1 INTRODUCTION

The requirements of this project are a voltage probe that has a frequency response to 40GHz and will minimally load a circuit on a CMOS substrate. The probed voltage is to be displayed on a high frequency oscilloscope.

In commonly used measurement techniques the general characteristics of an electrical probe have been to measure a voltage signal in the time domain. The desirable characteristics of such a probe are that the probe should not influence or load the response of the circuit under test. It should provide an accurate although perhaps attenuated representation of the probed signal over a range of frequencies. These characteristics require that a voltage signal probe have a high resistance and low capacitance.

Technology is driving ever higher frequencies of circuit operation using smaller device sizes. With high frequencies and large on chip impedances, probing internal nodes is a challenge. Typical probe devices have a much lower impedance than the device under test. To measure these nodes a voltage signal probe must have a high resistance and ultra low capacitance.

Conventional voltage probes use a resistor / capacitive divider to minimize probe input capacitance on the load [1]. This works well at low frequencies, but internal resistors and capacitors of a conventional probe have parasitic impedances that distort frequency response at GHz frequencies. Additionally, low impedance of a probe with a several pico-Farad input capacitance can load a high impedance node, causing circuit failure.

At frequencies in the GHz range, parasitic inductances and capacitances of an electronic component dominates the effect of the device. Because of the parasitics, even the smallest of surface mount devices (SMD) components have a resonance frequency in the medium GHz range [2]. Component selection is critical to performance at GHz frequencies. All devices have a parasitic

component. A method to de-embed the non-idealistic performance of a voltage probe constructed from non-idealistic components is presented.

For a voltage probe to be effective at GHz frequencies, a combination of characteristics is appropriate. First, the input capacitance needs to be much less than the few pico-Farad value of a standard probe. Second, parasitic impedances caused by physical size of the probe components should be minimized. Lastly, a correction component needs to be added to the probe to restore a flat frequency response.

Abandoning the resistor divider portion of a probe, the ability to measure a DC voltage is lost. But this eliminates parasitics associated with these components. By designing an ultra low value capacitor as part of a probe tip, parasitic components associated with a capacitor can be minimized as well as the loading effects of a probe with a larger value capacitor.

Current through a capacitor is expressed as the derivative of the input signal (1). The output current is viewed as a voltage across a terminating resistor (Fig. 1). Using a capacitive input probe, part of the correction component will need to be an integrator.

$$\text{Current through a capacitor} \quad i = C \frac{\delta V}{\delta t} \quad (1)$$

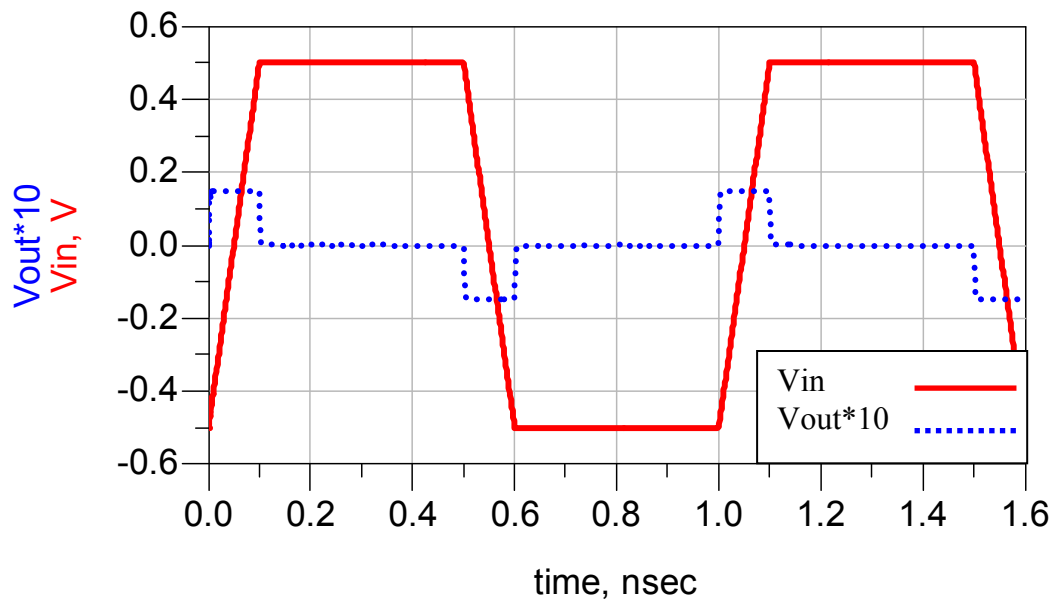


Fig. 1 Voltage vs. Time for a 1 GHz Input Signal and Ideal Probe Output. The probe output is the derivative of the input signal. Using the probe output, the rise-time and frequency can be determined. Rise time is expressed by the width of the output pulse and frequency expressed by the reciprocal of the time between like polarity pulses.

Probing internal nodes in integrated circuits is often required in trouble shooting designs. Tungsten probe needles can be sharpened to nanoscale dimensions to allow probing sub-micron circuits. Passivation on integrated circuits can be removed by a focused ion beam (FIB). The tungsten probe can be placed on an internal node or a deposited pad built up by a FIB. These internal nodes can only drive small capacitive loads of the order of several 10's of a femto-Farad (fF). The RFIC probe is designed for such applications. The tungsten needle and the center conductor of a coaxial cable are designed as a capacitor. This provides the means to create an ultra low value capacitor. By utilizing a simple design, input impedance is maximized and parasitic components are minimized (Fig. 2).

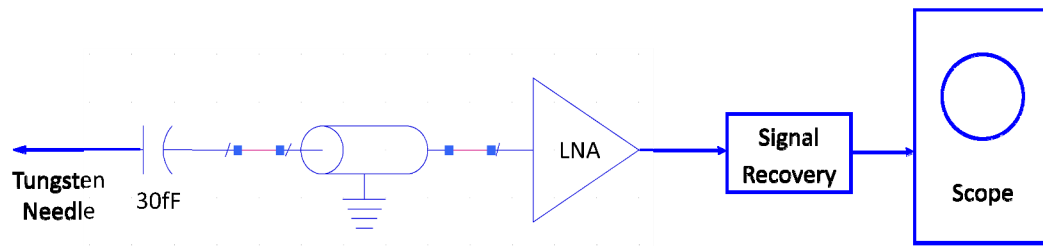


Fig. 2 Block Diagram of the Ultra Low Capacitance RFIC Probe.

The mutual capacitance between the whisker and the coaxial center conductor is designed to be 30fF.

1.1 Thesis Outline

This thesis is divided into 8 sections. The first section contains the required pretext pages. Chapter one is the introduction. Chapter two (Prior Art) is a comparison of prior art and high frequency performance. Chapter three (RFIC Probe Design) discusses the design procedure. Construction details and circuit analysis are performed. Chapter four (RFIC Probe Characterization) develops a transfer function of the manufactured probe. Chapter 5 (High Frequency Test Circuits) designs two sensitive oscillator circuits and a 22 nm inverter for probe testing. Chapter six (Measurements and Signal Recovery) explains the method to use simulated circuits combined with the extracted parameters from the manufactured RFIC probe to derive the correct input signal. Additional measurements are taken on a real circuit and the input signal is recovered as well. Chapter seven is the conclusion. The appendix contains design specifications and programming scripts.

2 PRIOR ART

2.1 Introduction

Voltage measurement probes fall into several categories. Low impedance (50 Ohm) probes generally have good high frequency performance. High impedance probes generally have poorer high frequency performance but have the advantage of not significantly loading the device under test. Non contact probes typically use either proximity or optical means to collect data. Table 1 shows the variety of voltage probes and their limitations.

Table 1
Voltage Probe Variety

Probe Type	Frequency Response	Limitations
Passive [3]	Up to 500MHz	11pF input cap loads high frequencies on DUT
Active / Low Capacitance [3]	Up to 6GHz	500fF input cap loads high frequencies on DUT
High voltage probes [4]	Up to 250MHz	11pF input cap loads high frequencies on DUT
Driven Shield [4]	Up to 1GHz	50 Ohm input resistance and 1pF cap loads DUT
RF Probe [5]	Up to 240GHz	50 Ohm input resistance loads high impedance DUT
RF Probe [6]	Up to 40GHz	50 Ohm input resistance loads high impedance DUT
Hi Impedance [6]	Up to 26GHz	1.25 M Ohm and 50fF is similar to the RFIC probe.
Non Contact Capacitive Coupled [7], [8], [9]	Up to 30GHz	Sensing array and DUT must be designed for alignment.
Laser Voltage Probe (LVP) [10]	Up to 10GHz	Unknown amount of capacitive loading. Complex system
Mixer Probe [11]	20GHz	50 Ohm input resistance loads high impedance DUT
Electro Optic [12]	Not applicable	Signal is injected, not measured

2.2 Comparisons of Probes

Passive voltage probes are the most common type of oscilloscope probe (Fig. 3). Varieties include 1X, 10X and 100X type probes. The X refers to the voltage reduction of the probe with 10X being the most common [1]. Standard 10X probes utilize voltage division using both resistive and capacitive means. A low pF variable capacitor is in series with the capacitance of the measuring instrument. Probe input capacitances are 2-15pF with the 10X models and about 3pF with the 100X models [1]. The impedance of a probe is expressed by (2).

$$\text{Parallel Impedance} \quad Z = \frac{R * \frac{1}{j\omega C}}{R + \frac{1}{j\omega C}} \quad (2)$$

Using the Tektronix probe in Fig. 4, where R is equal to 10Meg Ohms and C is equal to 11pF gives an impedance of 144 Ohms at 100MHz. Even at medium MHz frequencies this low of impedance will overload internal IC nodes.

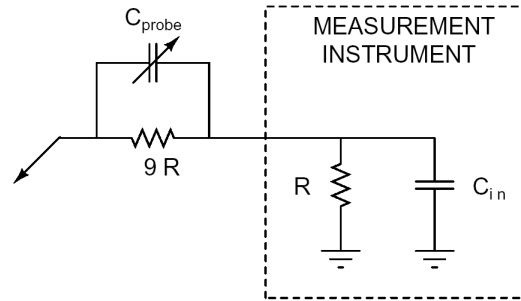


Fig. 3 Circuit Diagram of 10X Voltage Probe.

The input signal is reduced 10X by the resistor divider. Because the measurement device has finite input capacitance, a capacitor divider is also needed with C_{probe} having one ninth the value of C_{in}. The zero caused by C_{probe} is adjusted to cancel the pole caused by C_{in}.

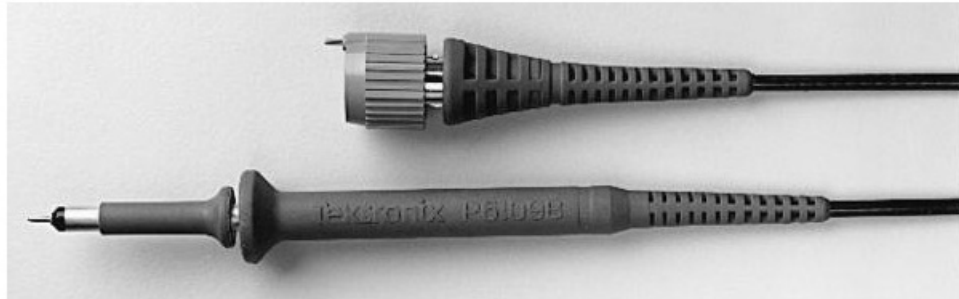


Fig. 4 Passive Oscilloscope Probe.

This probe has a frequency response of 500 MHz [3]. Input impedance is 10M Ohms with a loading capacitance of 11pF.

Active probes [13], [3] (Fig. 5 and Fig. 6) generally have a field effect transistor (FET) input configured in a source follower type circuit. The FET is positioned close to the probe tip to minimize probe capacitance. The source follower circuit amplifies signal current while maintaining bandwidth close to the cutoff frequency of the transistors.

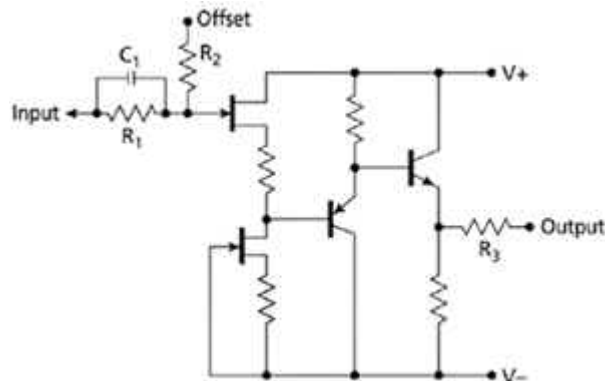


Fig. 5 Active Oscilloscope Probe.

This probe uses a source (emitter) follower circuit [14]. Follower type circuits supply current gain without voltage gain. Due to the absence of voltage gain, the circuit has maximum bandwidth because of the Miller effect.



Fig. 6 Active Oscilloscope Probe.

This probe has a frequency response of 6GHz [3]. Input impedance is 20k Ohm with a loading capacitance of $\sim 500\text{fF}$.

High voltage probes (Fig. 7) utilize both resistive and capacitive dividers in their design [15], [16]. High input capacitance is particularly problematic in these designs. Of interest to this work, by eliminating the large high voltage resistors, the high frequency performance of the probe improves at the expense of DC usefulness.



Fig. 7 High Voltage Probe.

This probe has a frequency response of 1GHz and voltages to 5KV [4].

To reduce input capacitance, and the respective circuit loading, a technique of driving the shield with a buffered input signal (Fig. 8) is sometimes used. Reducing the potential difference between the shield and the center conductor of the input coax, minimizes associated capacitance. The buffering amplifier is placed close to the probe tip in a positive feedback configuration. To prevent oscillation, the amplifier supplying signal to the shield must be much faster than the frequency of interest. Thus, the shield amplifier limits frequency response to this type of probe.

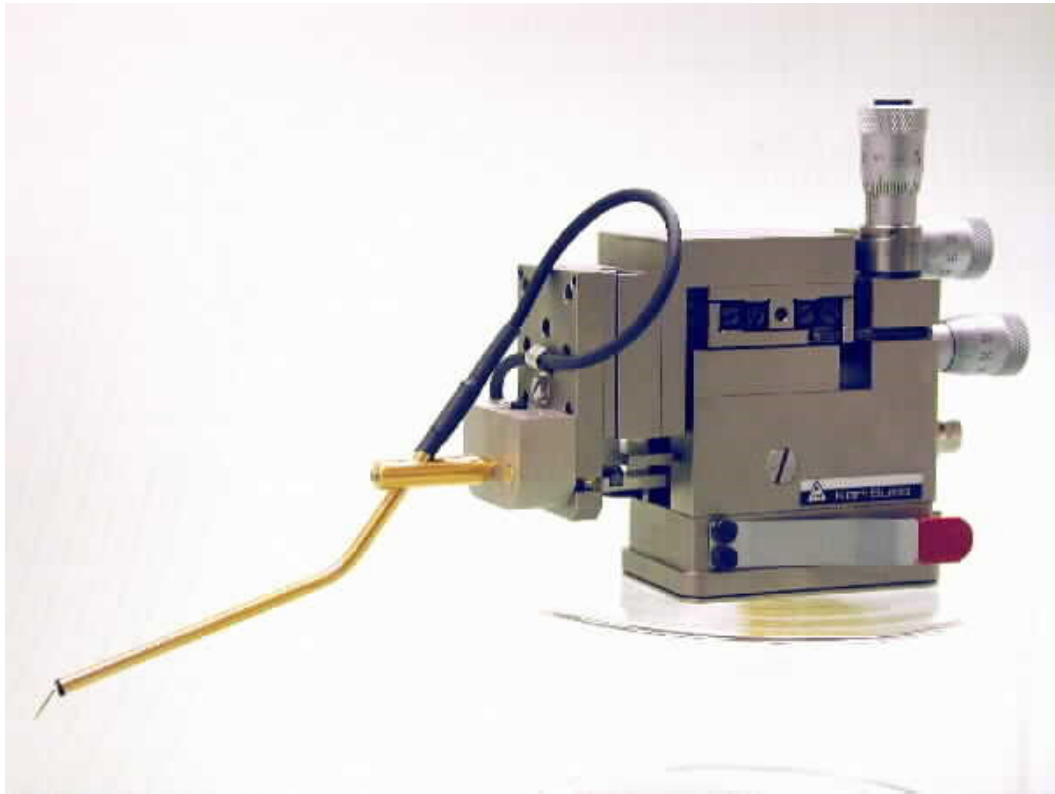


Fig. 8 Active Shield Probe with Micro-Positioner [4]. Frequency response is 1GHz. Input impedance is 50 Ohms with a loading capacitance of less than 1pF. The input signal is placed on the shield in a positive feedback configuration, reducing input capacitance.

RF probes (Fig. 9) are designed for a 50 Ohm impedance interface [5]. The probe tip is configured as a 50 Ohm coplanar waveguide [17] enabling impedance matching. To use these probes, a 50 Ohm buffer stage with a impedance matching probe landing zone is designed at the chip level. 50 Ohm matching is continued from probe contacts through the probe and cable to the test instrument. Reflections caused by impedance mismatch are minimized by this design. This probe type is used as a reference in testing the ultra low impedance RFIC probe.

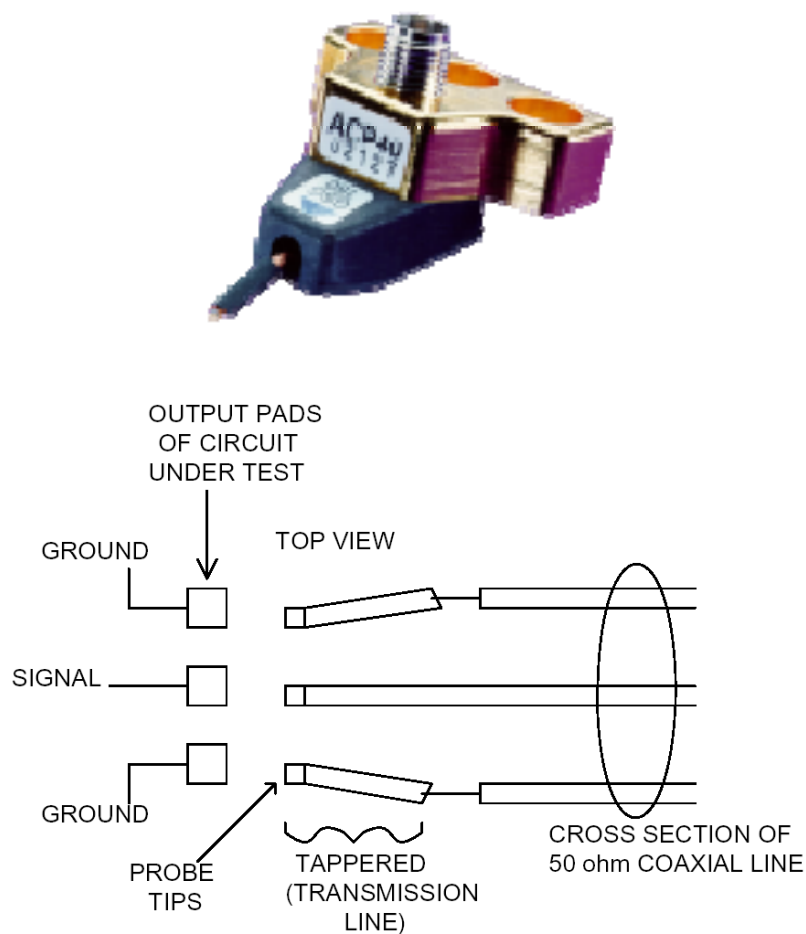


Fig. 9 GSG Type RF Probe.

The probe tip is manufactured as a 50 Ohm transmission line (coplanar waveguide) to facilitate matching probe tip to specially spaced output pads [5].

This research began by request of sponsors to improve the performance of the Picoprobe Model 35 (Fig. 10 and Fig. 11). This probe is designed to measure high frequency signals at high impedance nodes. This probe uses only a single contact and does not require a ground contact. The return path is accomplished by stray capacitance. The assumption is that this capacitance is much lower impedance than the probe itself.

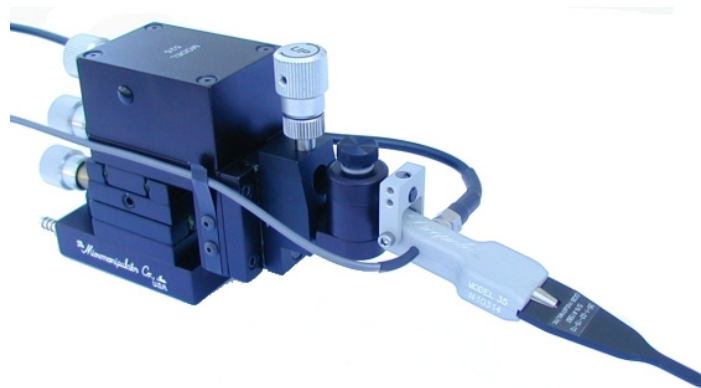


Fig. 10 High Impedance Probe.
Frequency response is 26GHz [6]. Input impedance is 1.25 M Ohms with a loading capacitance of 50fF.

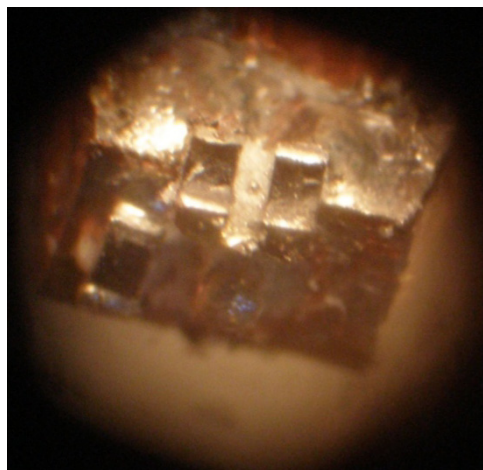


Fig. 11 Photo of High Impedance Probe.
Reverse engineering a high impedance probe. This probe utilizes a RC network similar to Fig. 3, with an amplifier built into the probe. The amplifier does not compensate for the parasitic effects of the SMD components.

Fig. 12 illustrates a non-contact capacitive coupled probe [9] . This type of probe requires mechanical alignment between the sensing array and the device under test. Because of the alignment requirements, its suitability may be best in high volume production testing.

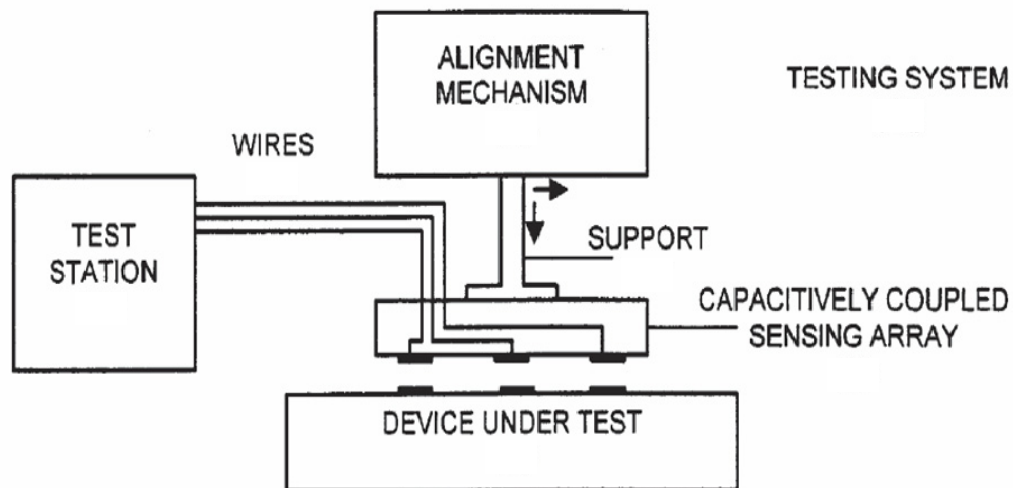


Fig. 12 Capacitive Coupling.

With non contact probing [7], [8], [18], there is a capacitive coupling that may be hard to quantify. The DUT will need to be physically designed to work with the sensing array.

Fig. 13 illustrates scanning probe microscopy (SPM) techniques [19], [20], [21] and [22]. The SPM probe operates by sensing electrostatic force. Induced mechanical deflection of a micro-fabricated probe as it responds to the localized circuit-probe Coulomb force caused by a potential difference.

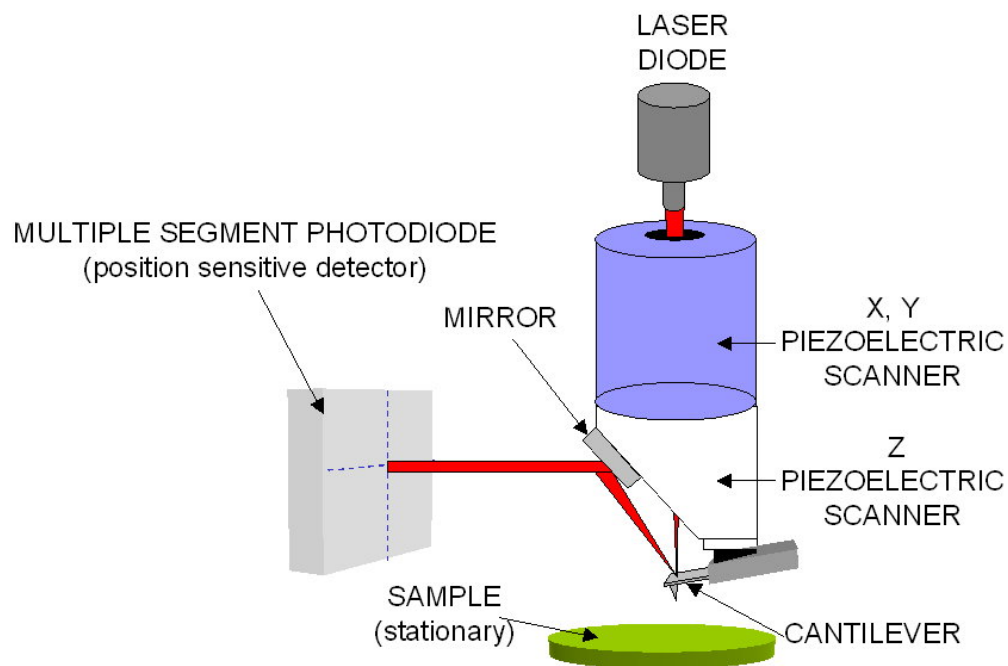


Fig. 13 Laser Voltage Probe (LVP).

A novel optical probing technology for flip-chip packaged micro-process [10].

Other high frequency probes [23], [24] have discrete components for the divider that gives the corner frequency of $\sim 15\text{GHz}$. Mixer type probes are built on a semiconductor substrate. [11] A local oscillator and mixer are used to down-convert the signal of interest to a lower frequency that is measured by standard test equipment. Disadvantages of this are the complexity of the circuit, trouble achieving a wide bandwidth with tuned components and the scaled frequencies to be measured. Electro-Optic [12] probes offer another avenue of probing. This technique uses a focused laser to bias or switch internal nodes of a MOS circuit. Instead of measuring a signal, this type of probe injects a signal into the DUT. Other electro-optic probes that detect the down-converted energy by mixing the microwave signal from an RFIC with laser energy from the probe. [25], [26].

3 RFIC PROBE DESIGN

3.1 Introduction

Resistors, capacitors, and inductors all have parasitic components that will create a resonance at a particular frequency [25]. Even the smallest size 0402 surface mount device (SMD) resistor will have sufficient capacitive and inductive parasitics to create a resonance in the medium GHz frequencies. For this reason, it is decided to eliminate resistors in the design and utilize a capacitive coupled probe.

The heart of the probe is the ultra low value capacitor. It is designed as the capacitance between a tungsten needle and the center conductor of a micro-coaxial cable.

3.2 Design Goal

The goal in designing the RFIC probe is to minimize the parasitic components and the corresponding adverse frequency response. An effort is made to push major resonance components to or above the frequency of interest. Also, the quality factor (Q) of the probe is set as low as possible to soften the resonances, This will improve the linearity of the probe. Knowing that the probe response will not be linear, an algorithm will be used to fix or de-embed the probe response. Mechanically, the probe design will be to make the probe as thin and streamline as possible. This will enable better viewing of the circuit under test in a probe station microscope.

3.3 Probe Tip Design

To meet the requirements for RFIC probing, the probe tip needs to be designed small enough to probe sub-micron circuits and durable to withstand repeated use. Tungsten needles are commonly used for this application. An industry standard 16 micron needle with a sharpened tip is selected for this purpose.

The tungsten needle can be modeled as a coaxial line with the shield being the ambient metal surroundings of a probe station. Using the coaxial capacitor and inductance per unit length formulas (3) and (4), the characteristic impedance (Z_o) of the needle is derived using (5), where a is the inner conductor radius and b is the shield radius [27].

$$\text{Coaxial conductors} \quad C = \frac{2\pi\epsilon}{\ln \frac{b}{a}} \quad (3)$$

$$\text{Coaxial conductors} \quad L = \frac{\mu}{2\pi} \ln \frac{b}{a} \quad (4)$$

$$\text{Characteristic impedance} \quad Z_o = \sqrt{\frac{\mu}{\epsilon}} \frac{\ln \frac{b}{a}}{2\pi} \quad (5)$$

$$\text{Wavelength} \quad \lambda = \frac{c}{f} \quad (6)$$

With the a needle radius (a) being 8 microns and the surroundings (b) at several centimeters, the air coax formed by the needle is 470 ohms (Fig. 15). The several centimeter radius is not a critical dimension for a stable 470 Ohm transmission line. With a 470 Ohm transmission line connected to a capacitor, reflections will occur at all frequencies except where the transmission line impedance is matched to the capacitive reactance of the coupling capacitor. In an effort to minimize reflections, the length of the needle is selected (6) to be shorter than a quarter wavelength ($\lambda/4$) up to the maximum measured frequency. The quarter wavelength of 40GHz is 2mm. This measurement is selected for the needle length.

3.4 Capacitor Design

Circuit loading depends on the coupling capacitance. The coupling capacitance is balanced to a value that will minimally load the device under test

(DUT) but still capture enough signal for measurement at the GHz frequency range of interest.

A workable input impedance of 500 Ohms is desired at 10GHz. Assuming a negligible resistance, capacitance can be calculated (7) as 30fF. The capacitor is configured as a gap between parallel wires consisting of the tungsten needle and center conductor (Fig. 14). To calculate the capacitance of wires with different diameters, a series combination of a coaxial capacitor (C_1) and a capacitor consisting of parallel conductors (C_2) is required [27]. Equations (3) and (8) are combined by (9). In the parallel wire capacitance per unit length formula, (8) s represents the center to center spacing and b represents the inner coaxial radius.

Desired capacitance $C = \frac{1}{\omega Z}$ (7)

Parallel conductors $C_2 = \frac{\pi\epsilon}{\ln \frac{s}{b}}$ (8)

Series combination $C = \frac{C_1 C_2}{C_1 + C_2}$ (9)

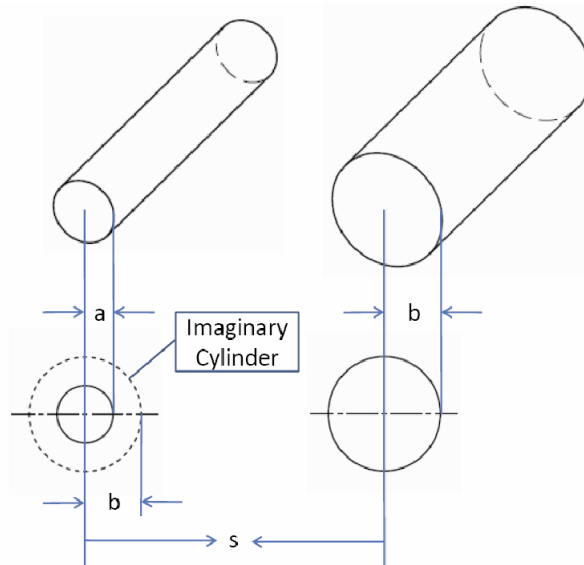


Fig. 14 Deriving the Capacitance Between Dissimilar Conductor Sizes.

The smaller cylinder represents the tungsten needle. For the purposes of the calculation it is surrounded by an imaginary cylinder of the same size as the coaxial inner conductor [28].

3.5 Preliminary Probe Calculations

Putting the needle and coupling capacitances of the previous section together, an initial circuit is put together. Semi-rigid coax UT-47-M17 by Micro-Coax is selected due to its cut off frequency in excess of 130GHz [29].

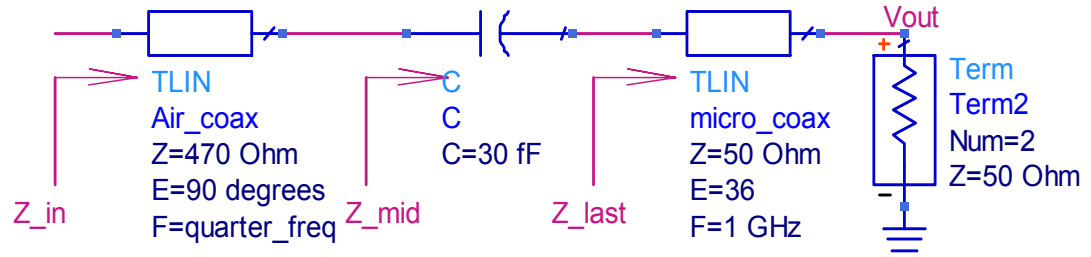


Fig. 15 Test Schematic to Optimize Needle Length and Coupling. Input impedance is solved both by hand and by Agilent Advanced Design System (ADS) circuit analysis.

To solve this circuit, velocity of propagation (V_p), electrical length (θ) and beta (β) is solved for the Micro-Coax (10), (11) and (12). These values plus the 50 Ohm Z_L termination impedance is used to calculate Z_{last} (13). Z_{mid} is the sum of Z_{last} plus the impedance of derived desired capacitance (C) (7). Lastly Z_{in} is calculated by using the same methodology as solving for Z_{last} but using Z_{mid} in place of Z_L termination impedance.

$$\text{Velocity of propagation} \quad V_p = \frac{c}{\sqrt{\epsilon_r}} \quad (10)$$

$$\text{Electrical length} \quad \theta = 360^\circ \frac{V_p * l}{f} \quad (11)$$

$$\text{Beta} \quad \beta = \frac{2\pi f}{V_p} \quad (12)$$

$$\text{Input impedance} \quad Z_{in} = Z_0 \frac{Z_L + jZ_0 \tan(\beta l)}{Z_0 + jZ_L \tan(\beta l)} \quad (13)$$

$$\text{Transfer Function} \quad H(s) = \frac{Z_L}{Z_L + Z_{IN}} \quad (14)$$

Initial hand calculations are confirmed with Synopsys HSpice (Appendix D). Agilent Advanced Design System (ADS) is later selected as the simulation tool due to its extended RF capacity and ability to import S parameter (Touchstone) device models. Using Matlab, the hand calculations and ADS circuit analysis are plotted and are in agreement (Fig. 16). Both analyses reveal the input impedance of the idealized circuit of Fig. 15. Following the same hand analysis, a complete set of Z parameters could be derived for the RFIC probe. At frequencies below 1GHz the linear function of an ideal capacitor can be observed. The dip in impedance near 20 GHz is created by a resonance between the coupling capacitor and the needle. The peak near 40 GHz is from the destructive superposition of reflections created at a needle length of one quarter wavelength. The complete Matlab code is presented in Appendix E.

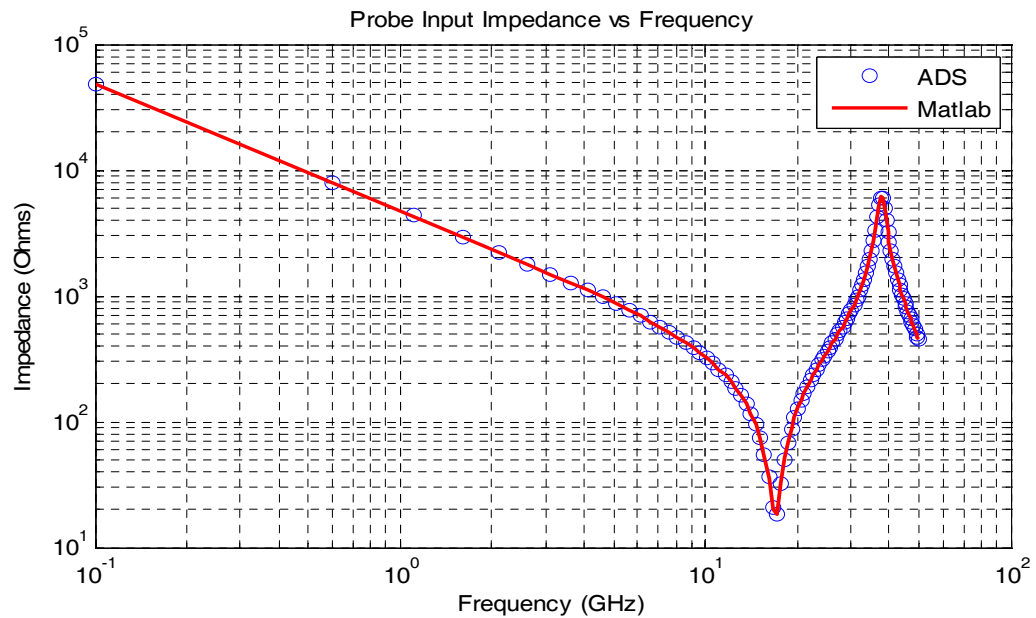


Fig. 16 Probe Input Impedance vs. Frequency.
Hand calculations performed in Matlab match the ADS test schematic simulation.

3.6 Probe Modeling

The preliminary calculations in the last section do not consider mutual inductive effects or fringe capacitance of the capacitive coupler. Neither does it consider the parasitic skin effect resistance of the tungsten needle. The probe is drawn in Agilent Electromagnetic Design System (EMDS) and simulated over a 40 GHz range. As with a network analyzer the simulator exports S parameters in a Touchstone format. The Touchstone file representing the modeled RFIC probe is imported into ADS. Simulations can be performed using the file as if it is a sub-circuit.

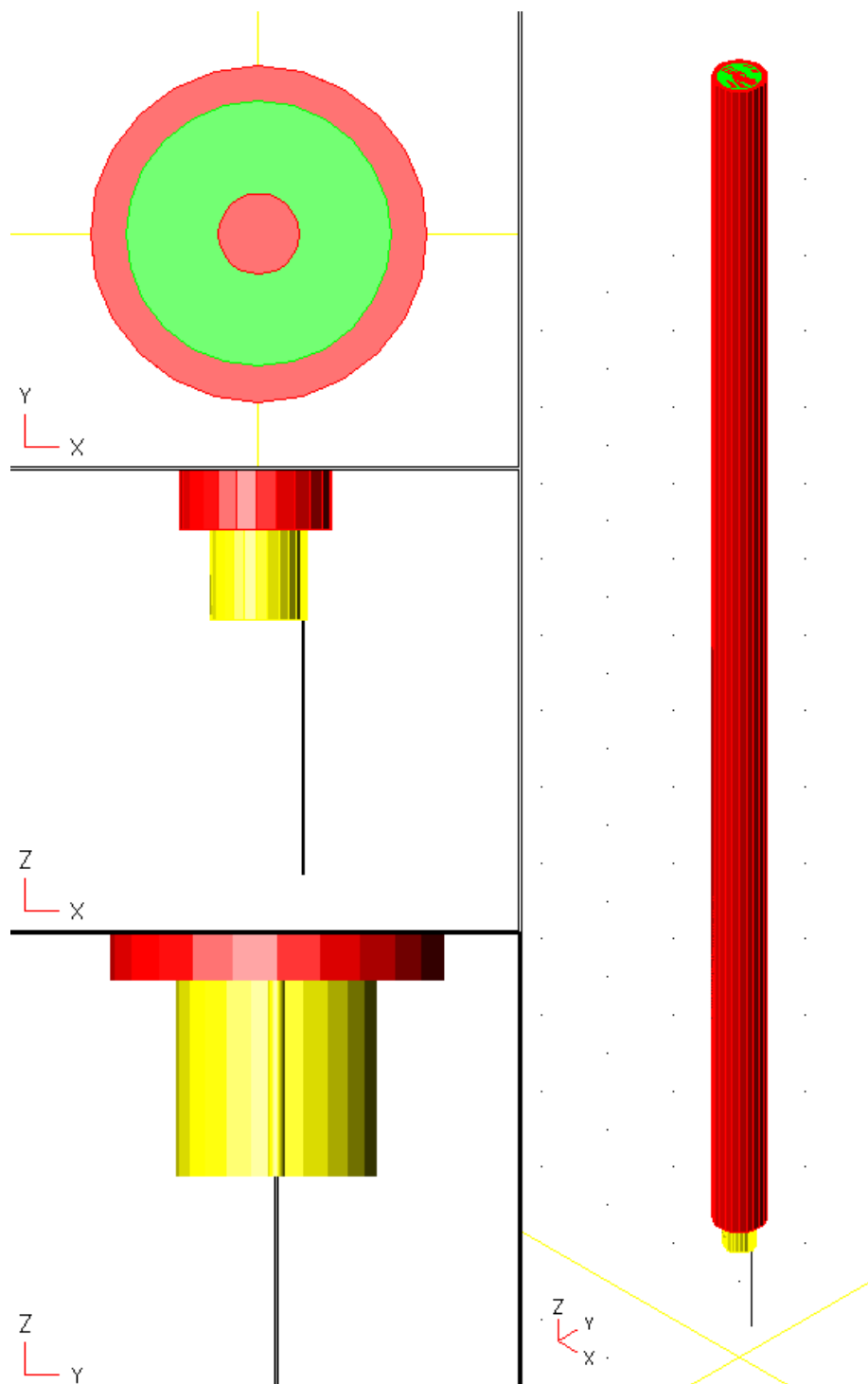


Fig. 17 EMDS Drawing of RFIC Probe.
The probe design is modeled using a EM solver. S parameters representing the probe are exported in a Touchstone format.

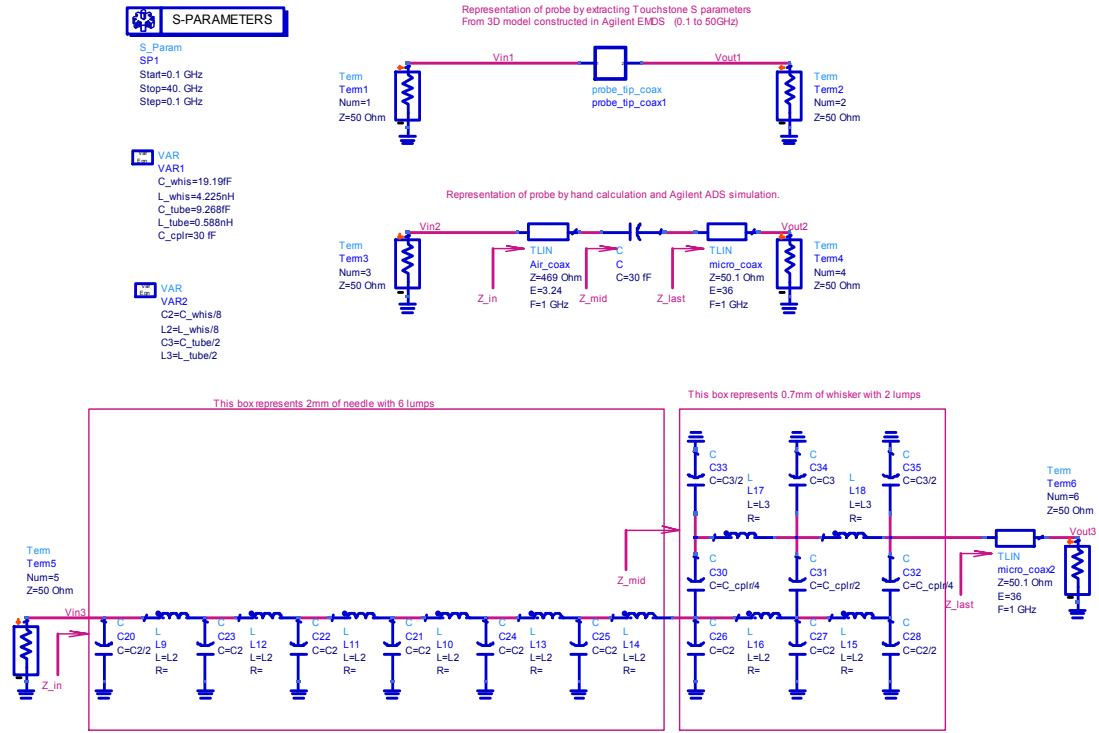


Fig. 18 Three Circuits Representing the RFIC Probe.

The sub-circuit box in the top circuit represents the EMDS extracted Touchstone file. The second circuit is a representation of the simplified circuit presented in the last section. The last circuit also includes a lumped element representation of the capacitor.

ADS is used to perform an S parameter simulation on the circuits of Fig. 18 (Fig. 19). In addition to the S parameters, the Z parameters are also extracted. Using Z parameters, the transfer function is extracted for all probe simulations [30]. Using an iterative approach, the needle length, coupling capacitance and center conductor is optimized for the placement and amplitude of the probe resonance frequency.

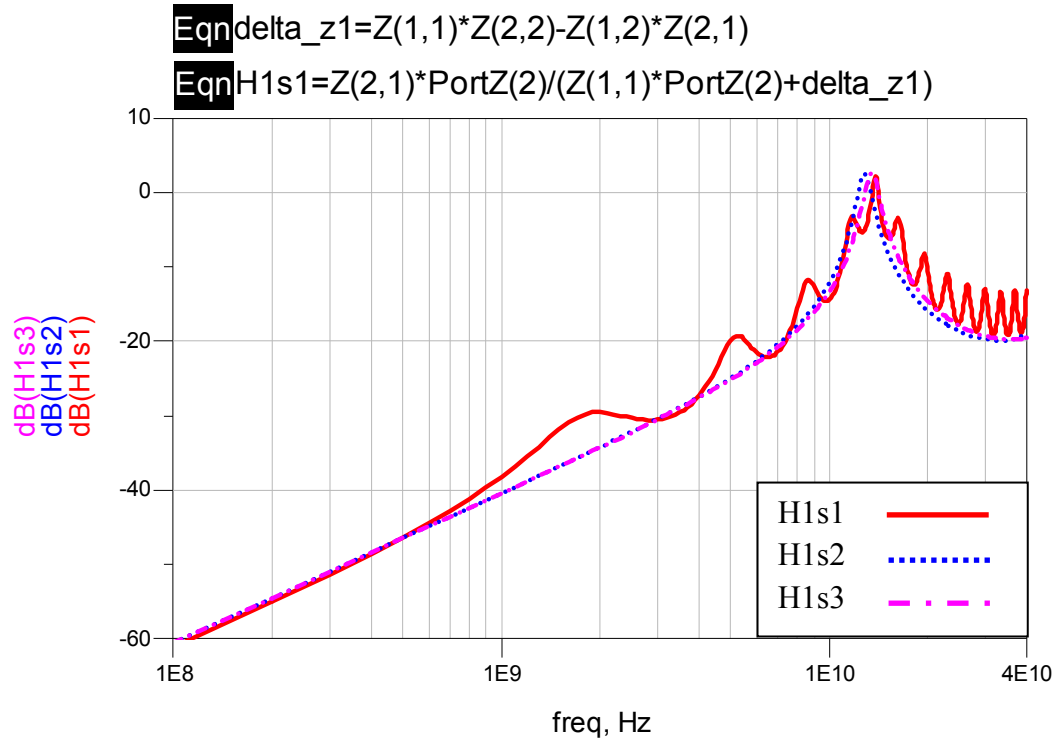


Fig. 19 Comparison of the Transfer Function.

The comparison represents all models presented in Fig. 18. To minimize reflections below 10GHz, terminal 1 impedance is matched to the needle impedance on all probes.

3.7 RF Connector

The upper frequency limit of a RF connector is dependent on several aspects [31]. High mechanical precision is required for a smooth transition from connector to the cable. This lowers voltage reflections at high frequencies caused by discontinuities. A medium with a low dielectric constant will cause lower dispersion. Ideally the connector will have air as the dielectric medium. Lastly, connector size is inversely proportional to its frequency response

A 2.92 mm connector is selected as the frequency response of this connector is in excess of 40GHz [32]. This is the same connector type used by the RF probes that will be used to characterize the RFIC probe. Additionally, 2.92mm connectors are thread compatible with less expensive SubMiniature version A (SMA) jacks for lower frequency applications.

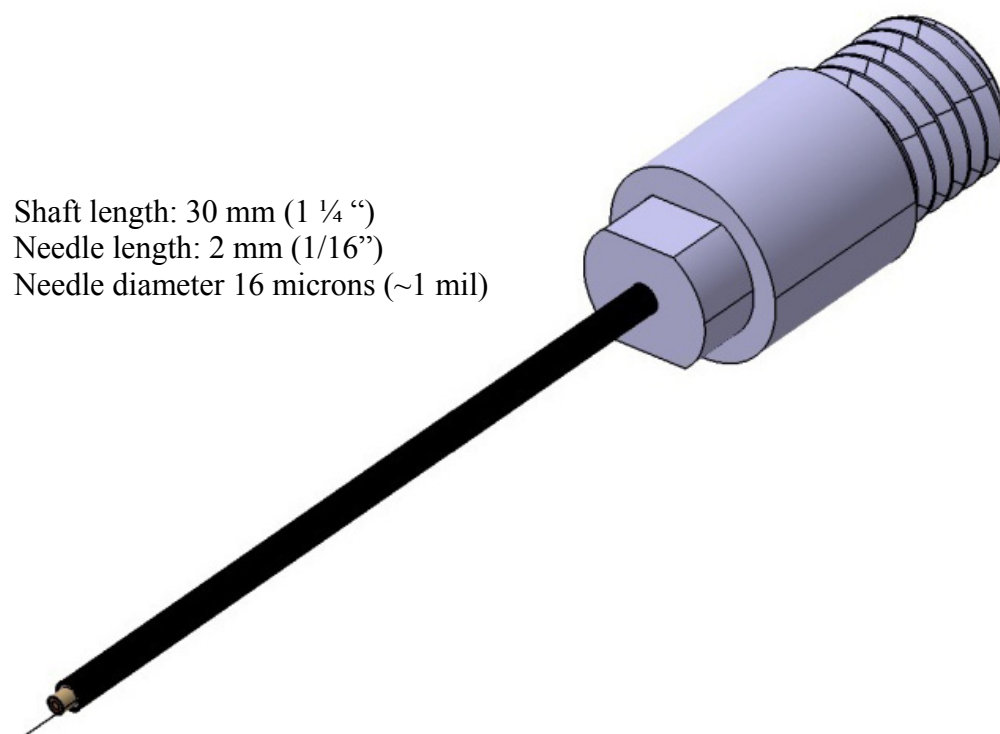


Fig. 20 Completed Probe Assembly.

4 RFIC PROBE CHARACTERIZATION

4.1 Introduction

Fig. 21 shows a square wave input signal and the RFIC probes representation of that signal. Note the delay in signal propagation and the differentiating action caused by the capacitive coupling. Also apparent is reflections caused by impedance mismatch the circuit under test and the RFIC probe. Clearly, further analysis will need to be done to recover the original square wave.

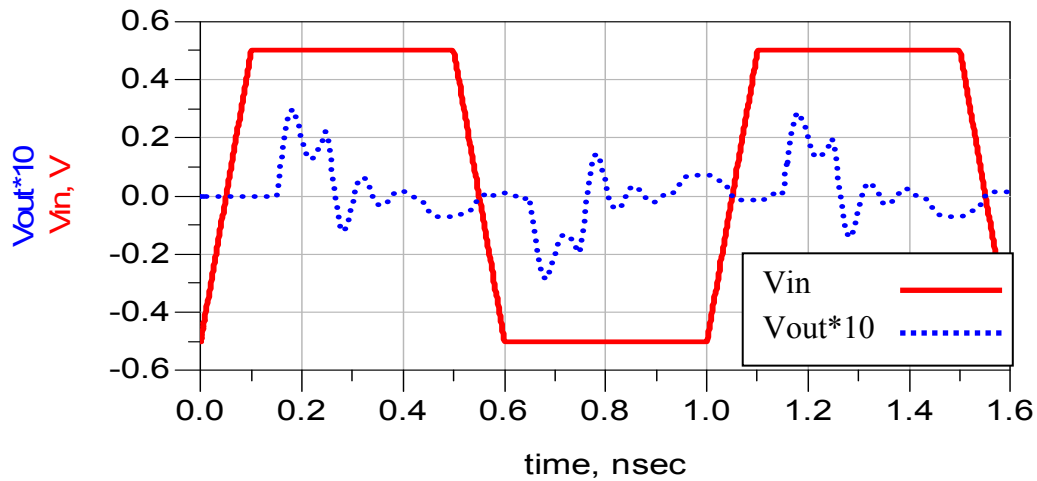


Fig. 21 RFIC Probe Input and Output Signals.

4.2 S parameter Analysis

Using two 50 Ohm GSG Cascade Microwave probes, a 50 Ohm GSG coupler on a Cascade test substrate a 40GHz vector network analyzer (VNA) is calibrated (Appendix C). The microwave probe connected to port 2 is replaced with the RFIC probe (Fig. 22).

An assumption is made that the second GSG microwave probe has a negligible effect on the VNA calibration. Six frequency sweeps are made from 0.1GHz to 40GHz in 50MHz steps (Fig. 23). The results are averaged and S parameters are saved in a Touchstone format.

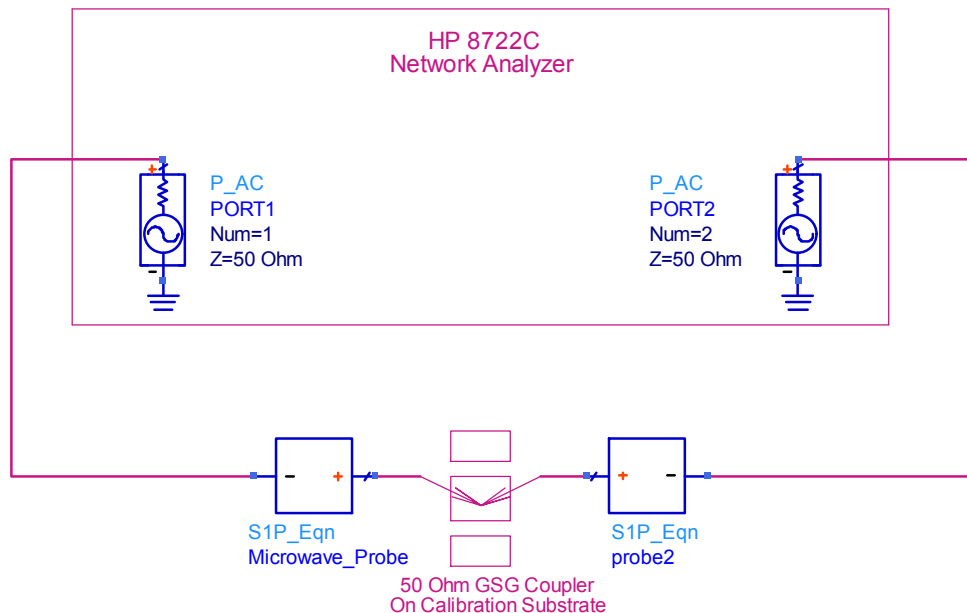


Fig. 22 VNA Setup for Probe Characterization.
The RFIC probe is analyzed from 0.1GHz to 40GHz and its S parameters are saved in a Touchstone file for later analysis with ADS.

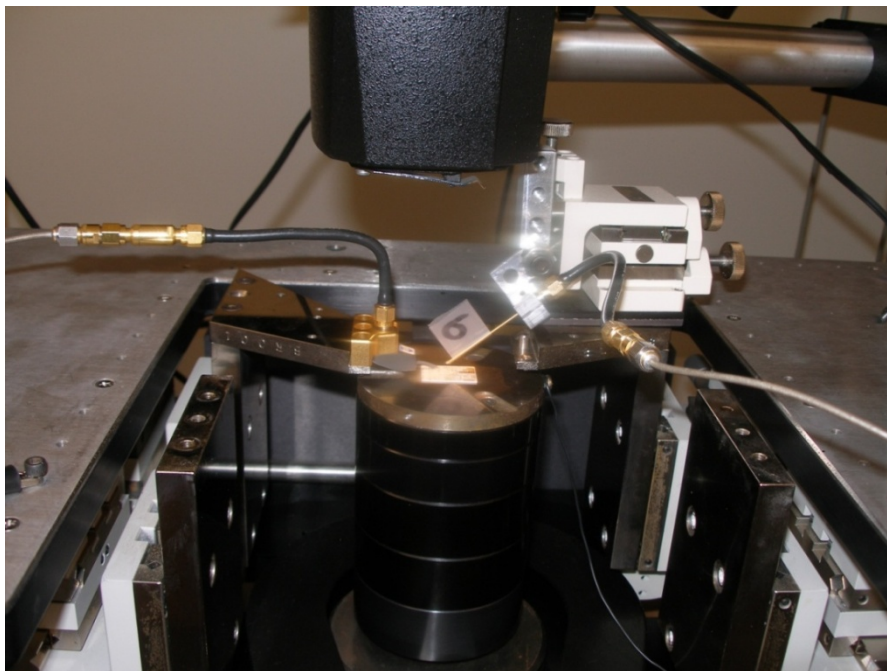


Fig. 23 Analyzing the RFIC Probe on a Probe Station.
The probe on the left is a 50 Ohm Cascade GSG RF probe. It lands on a Cascade test substrate and the probe on the right is RFIC probe.

4.3 Transfer Function

A transfer function is defined as the output of a device vs. frequency divided by the device input vs. frequency. Ideally, a probe would have a flat transfer function. If the probe does not have a flat transfer function, the transfer function itself can be used to mathematically flatten the probe response.

Two transfer function varieties are defined depending on what is to be achieved. $H1(s)$ (15) will allow V_{in} (The probe input) to be viewed given the probe output V_{out} (Fig. 24). However, probing sensitive internal nodes on ICs will adversely load the circuit. Using $H1(s)$, (15) the signal at V_{in} is viewed. This signal includes loading effects the probe has on the circuit.. Using $H2(s)$, (16) the signal at V_s is viewed. This is an advantage, as the node loading of the probe is accounted for in the transfer function. By adding the output impedance of the DUT to the probe transfer function, whatever loading the probe has on the circuit will be de-embedded. V_{in} is viewed as if the probe is not loading that node.

$$\text{Transfer function 1} \quad H1(s) = \frac{V_{out}(s)}{V_{in}(s)}$$

(15)

$$\text{Transfer function 2} \quad H2(s) = \frac{V_{out}(s)}{V_s(s)} \quad (16)$$

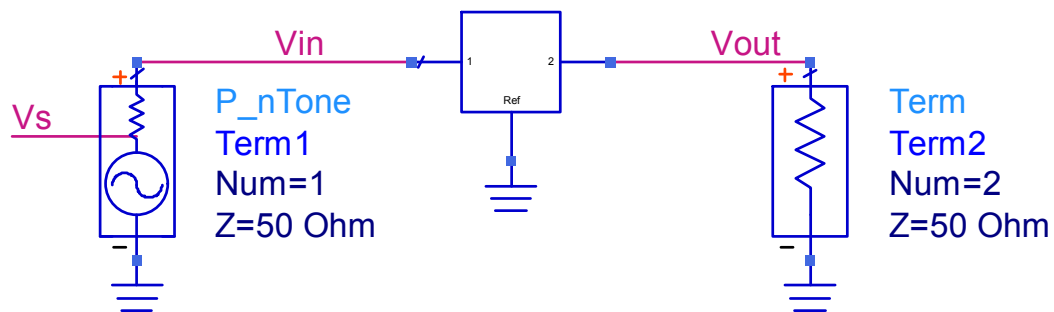


Fig. 24 Transfer Function Example.

The S parameters are converted to Z parameters then $H1(s)$ is extracted using (17) and (18) [30]. In the second case, we want to include the source impedance in the transfer function (Fig. 24). Dividing the probe frequency domain output signal by the frequency domain source signal reveals the transfer function, $H2(s)$ using S parameters (19) [33].

$$\text{Delta } Z \quad \Delta Z = Z(1,1) * Z(2,2) - Z(1,2) * Z(2,1) \quad (17)$$

$$\text{Transfer function 1} \quad H1(s) = \frac{Z(2,1) * Z_L}{Z(1,1) * Z_L + \Delta Z} \quad (18)$$

$$\text{Transfer function 2} \quad H2(s) = \frac{S(2,1)}{2} \quad (19)$$

Fig. 25 compares the transfer function of the 3D electromagnetic simulation of the RFIC probe and manufactured probe 2. Fig. 27 compares the transfer functions of manufactured probe 2. $H1(s)$ relates V_{out} back to V_{in} and $H2(s)$ relates V_{out} back to V_s .

With identical terminations at both terminals, an enhanced comparison of transfer functions would be to add 6dB to $H2(s)$ (Fig. 27). High frequency response is greater on $H1(s)$. The RFIC probe will load a node with a capacitance. With a high impedance node, this will create a low pass filter. $H2(s)$ having a lower high-frequency response will recreate the loaded signal at that node. Chapter 5 will explore this further.

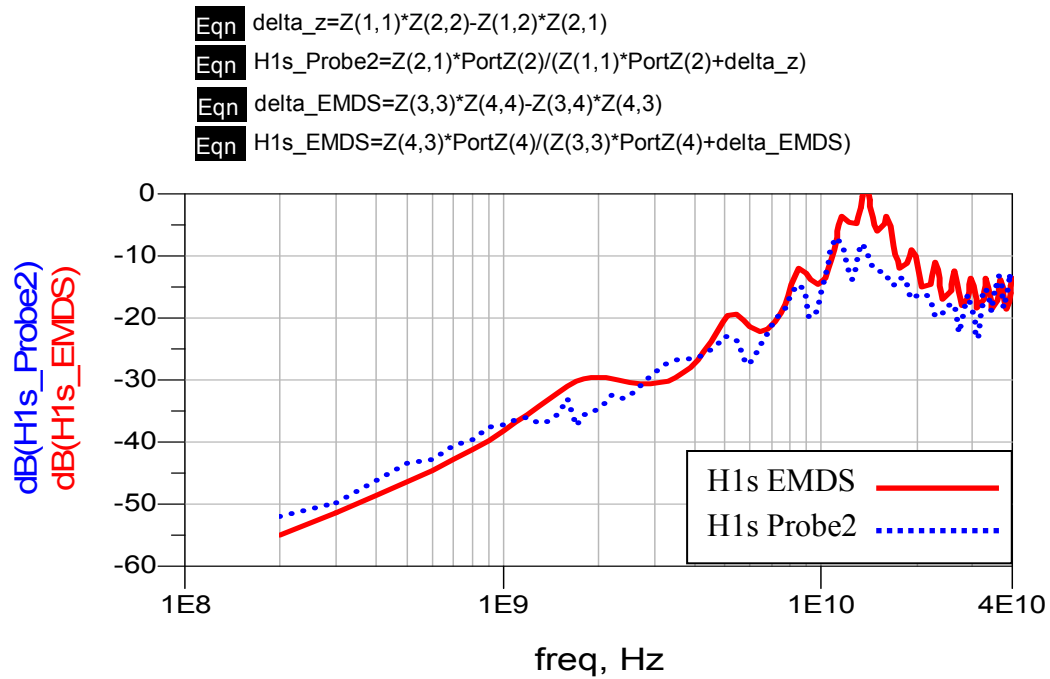


Fig. 25 H1(s) Transfer Functions of EMDS and Actual RFIC Probes. The input impedance is set at 50 Ohms. Note low frequency ripples caused by impedance mismatch between the source and the needle.

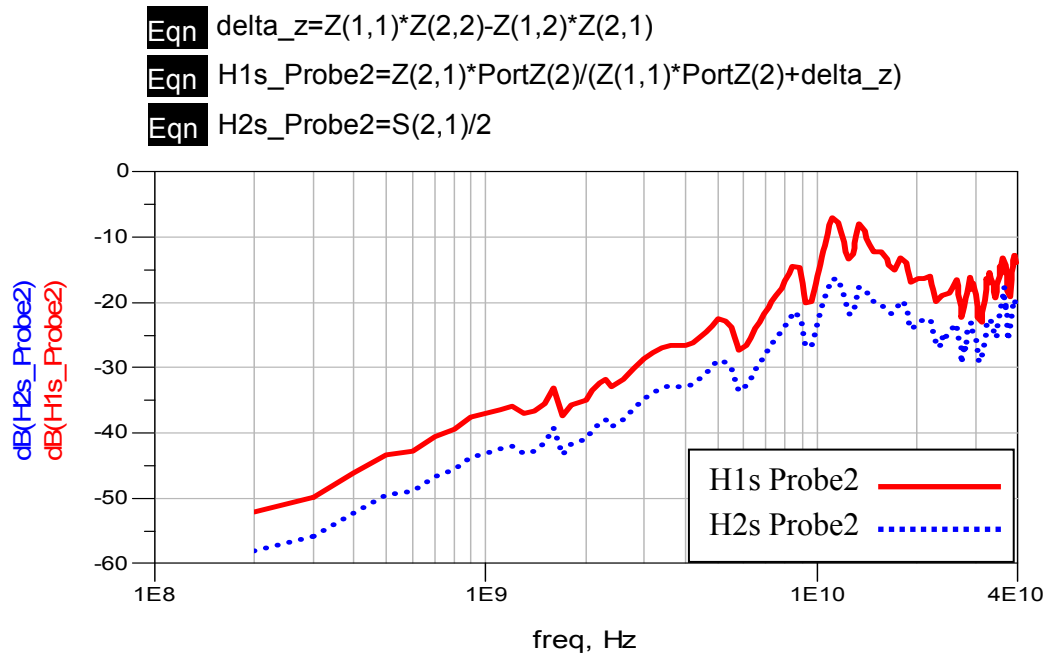


Fig. 26 Comparisons Between H1(s) and H2(s) Response. The amplitude difference between the transfer functions relates the amplitude between the source voltage, V_s and probe input voltage, V_{in} .

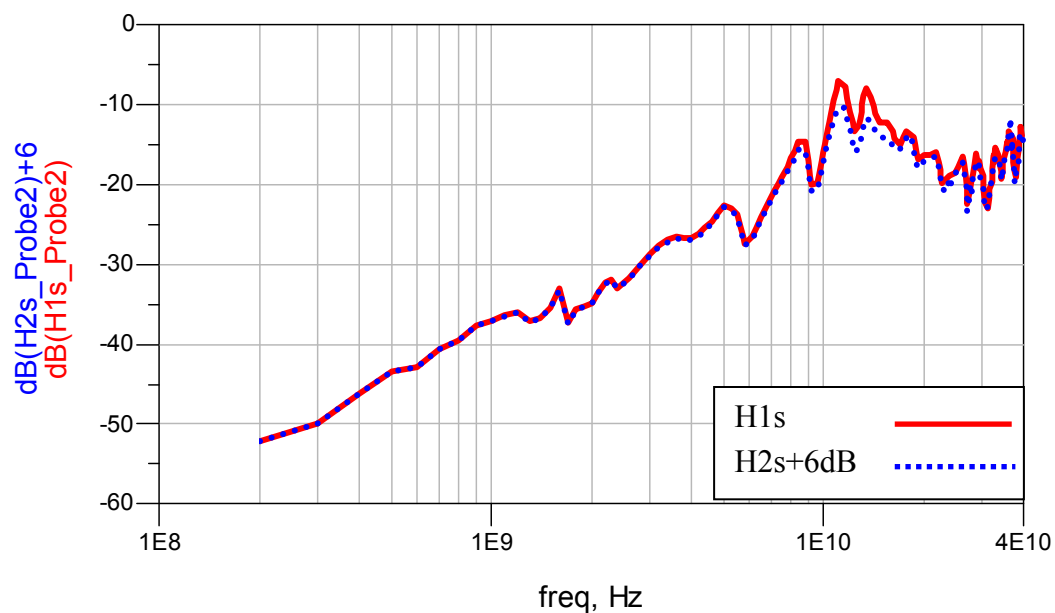


Fig. 27 Shifted H1(s) and H2(s) Comparison.

In addition to the amplitude difference, H1(s) has a greater high frequency response.

5 HIGH FREQUENCY TEST CIRCUITS

5.1 Introduction

To test the RFIC probe, several test circuits are designed [34]. These circuits are designed to have a high frequency signal at a sensitive high impedance node. Two oscillators are designed using a 0.18 μ m CMOS BSIM3 model. A Colpitts and a cross coupled oscillator are designed and modeled at 5.8GHz, which is the middle of the 5.7GHz band [35]. Both oscillators are designed for a loop gain of 2 using 0.8mA of current [34].

5.2 Colpitts Oscillator

A sensitive low power Colpitts oscillator is designed. The target frequency of oscillation is 5.8GHz. Letting $L=1\text{nH}$ and assuming a MOSFET parasitic capacitance of 200fF, the equivalent series capacitance of $C1$ and $C2$ (Fig. 5) is determined to be 0.583pF by (20). With a target N of 6, $C1$ and $C2$ is determined to be 0.7pF and 3.5pF respectively by (21).

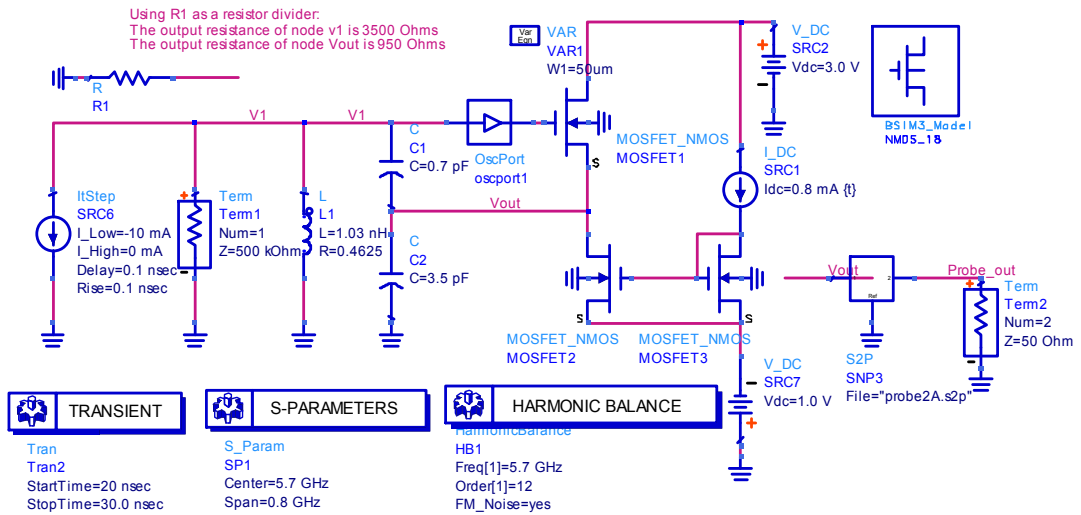


Fig. 28 5.8GHz Colpitts Oscillator.

The oscillator is shown with probe and load resistor. The load resistor is used to determine node resistance $v1$ and $Vout$ using a voltage divider equation.

$$\text{Frequency} \quad f = \frac{1}{2\pi\sqrt{LC_{equiv}}} \quad (20)$$

$$\text{Transformer ratio} \quad N = \frac{C1 + C2}{C1} \quad (21)$$

$$\text{Series Q} \quad \text{Series_}Q = \frac{\omega L}{R} \quad (22)$$

$$\text{Series Parallel} \quad R_p = R_s(1 + Q^2) \quad (23)$$

$$\text{Impedance Matching} \quad R_s = \frac{R_p}{N^2} \quad (24)$$

$$\text{Loop Gain} \quad \text{Loop_Gain} = N * \frac{gm * R_p / N^2}{1 + gm * R_p / N^2} \quad (25)$$

Series Q of the inductor with 0.46 Ohms of parasitic resistance is determined to be 79.2 by (22). A series parallel transformation determines $R_p=2900$ by (23). To use the gain calculation of a source follower, R_p must be moved to the source. This is done using the transformer formula by (24). Loop gain is given by the voltage gain of a source follower multiplied by N. By substituting the representation of R_s (24) into the source follower equation gives (25). By extracting gm from ADS, The loop gain is set at 2 with a width of 50um.

5.3 Cross coupled oscillator

A sensitive low power cross-coupled oscillator is designed (Fig. 29). With a width of 50um and a current of 0.8mA, C_{db} is extracted as 0.500pF. With a target frequency of 5.8GHz, L is determined to be 1.5nH using (26). Series Q of the inductor with 5.7 Ohms of parasitic resistance is determined to be 9.57 by (27). A series parallel transformation determines $R_p=556$ by (28). This gives a parallel tank circuit on the drain of M1 consisting of $L1$, C_{db} and R_p of 556. Transistor M2 also has an equivalent tank. For a loop gain of 2, the resistance looking down into M1, M2 should be one half R_p and is given by (29). With ADS, gm is extracted and R is determined to be 267 Ohms using an iterative process.

For both Colpitts and cross-coupled oscillators, the node impedance is determined by adding an external resistor at V1 and noting the voltage drop across the respective node. This is repeated for Vout. Using the voltage divider equation V1 is solved by (30). Solving for R2 gives the node impedance by (31).

$$\text{Frequency} \quad f = \frac{1}{2\pi\sqrt{LC}} \quad (26)$$

$$\text{Series Q} \quad \text{Series_}Q = \frac{\omega L}{R} \quad (27)$$

$$\text{Series to Parallel} \quad R_p = R_s(1 + Q^2) \quad (28)$$

$$\text{Node Impedance} \quad R = \frac{2}{gm} \quad (29)$$

$$\text{Voltage Divider} \quad V1 = V \frac{R1}{R1 + R2} \quad (30)$$

$$\text{Divider Rearranged} \quad R2 = \frac{V * R1}{V1} - R1 \quad (31)$$

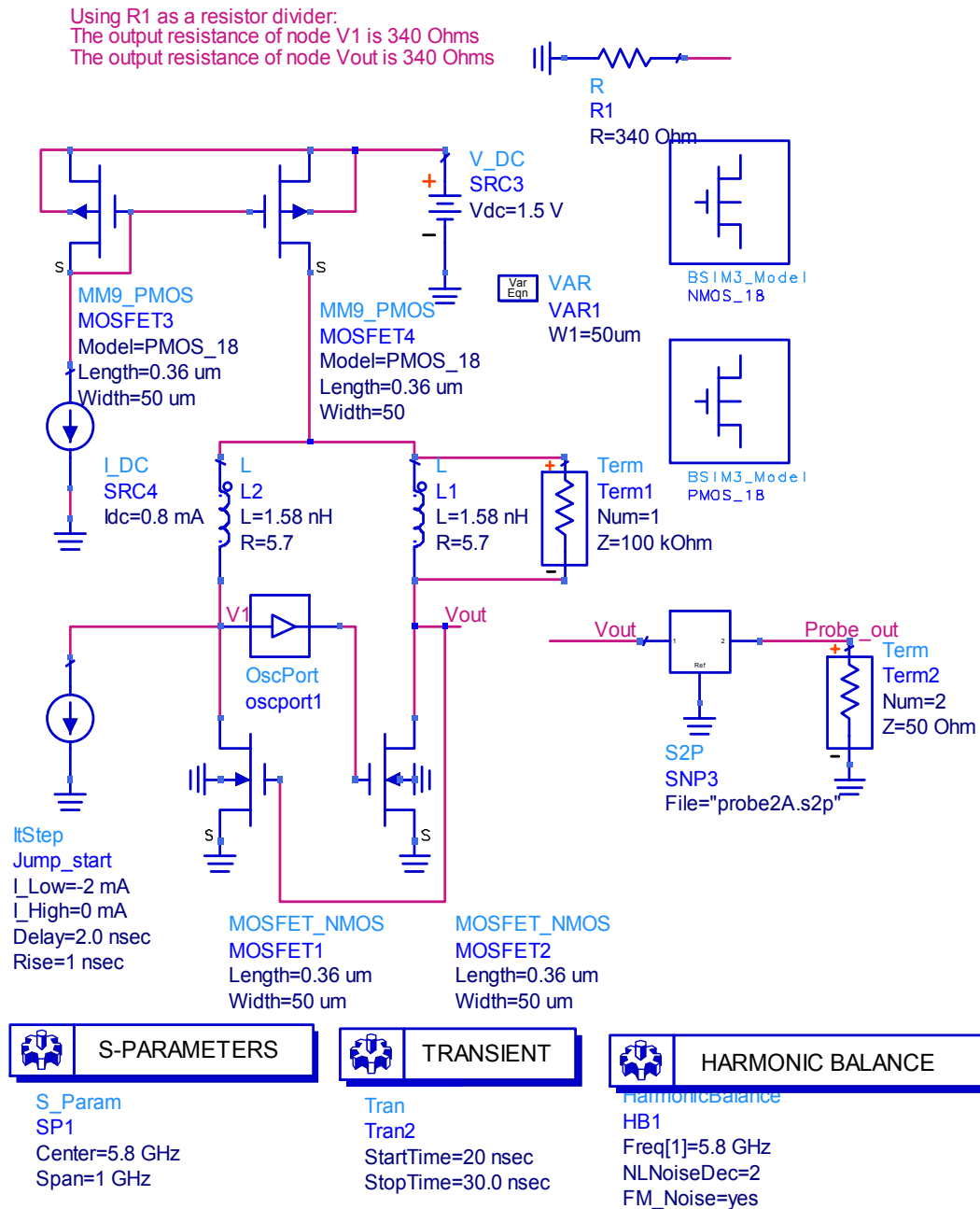


Fig. 29 5.8GHz Cross Coupled Oscillator.

The oscillator is shown with probe and resistor to determine node resistance. Parasitic drain capacitance is used as the tank capacitance.

5.4 22nm Inverter

Square waves are inherently more complex than sine waves because they are represented as the sum of an infinite number of sine waves in the frequency domain. Therefore the probe algorithm should be tested using a square wave. A sensitive low current 22nm inverter is designed based on a BSIM4 CMOS model. The input is a 10GHz signal with 20ps rise and fall times. The width of the PMOS and NMOS transistors are selected to be the same strength. Vout is the loaded output of the first inverter. As for the Colpitts and cross-coupled oscillators, the node impedance is determined by adding an external resistor at Vout and noting the voltage drop across the node. Using the voltage divider equation, Vout is solved by (30). Solving for R2 gives the node impedance by (31). Vout node impedance is verified by (32). Vout_not is checked during probing to ensure the second inverter is functional.

$$\text{Vout impedance} \quad R_o = \frac{1}{G_{ds}} \quad (32)$$

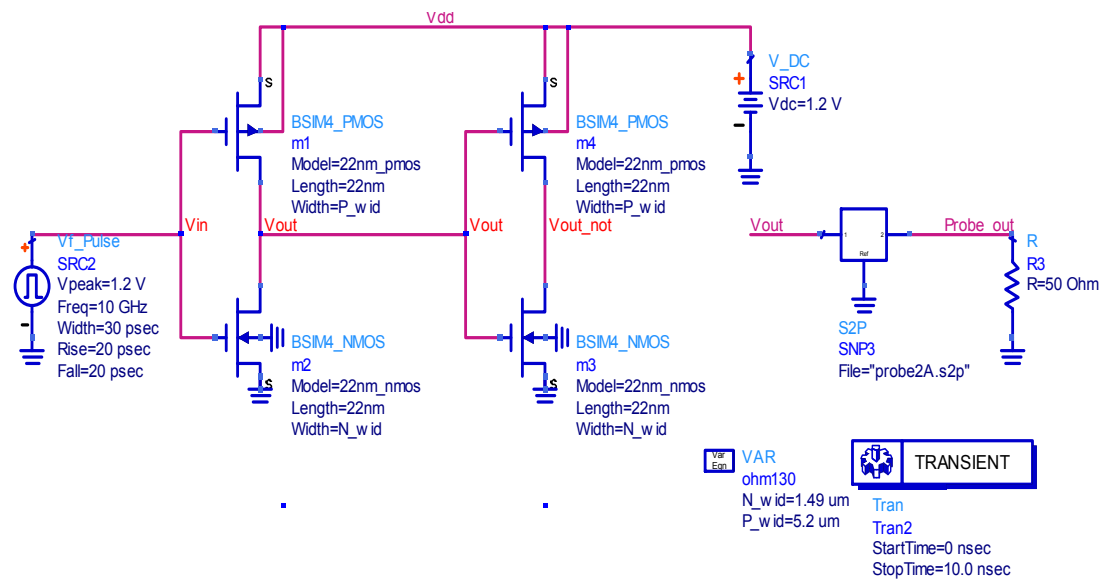


Fig. 30 Inverter Modeled From 22nm CMOS Process.

Vout is probed while Vout_not is checked to ensure the signal propagates to the second inverter.

5.5 Summary

The circuits in this section are designed with sensitive nodes. In the Colpitts oscillator, V1 has a high impedance. In the cross coupled oscillator, loop gain is selected at 2, a minimum design value. The 22nm inverter uses the shortest channel MOSFET model currently available [36]. Table 2 displays the impedances of the nodes that will be probed.

Table 2
Node Impedances of Test Circuits

Impedance of Node (Ω)			
Node	Colpitts Oscillator	Cross Coupled Oscillator	22nm Inverter
V1	3500	340	
Vout	950	340	130

6 MEASUREMENTS AND SIGNAL RECOVERY

6.1 Introduction

In this chapter, the internal nodes will be probed on the Colpitts and Cross-Coupled oscillators [34]. The 22nm inverter will also be probed. The manufactured RFIC probe is used to measure a 200ps rise time step. Using the derived transfer function and Fourier transforms, the input signal will be recreated.

6.2 Test Circuit Signal Recovery

When $H(s)$ was derived, the source impedance was matched to the DUT output impedance. All collected signals are sampled in time. The sampled time domain probe output signal is represented as $y(n)$. Next a fast Fourier transform (FFT) on the sampled time domain probe signal is performed (33), bringing it into the frequency domain $Y(k)$. $X(k)$ represents the output signal in the frequency domain (34) [37]. The time domain signal $x(n)$ can be recovered using an inverse fast Fourier transform (IFFT) (35).

$$\text{Frequency Domain Conversion} \quad Y(k) = FFT(y(n)) \quad (33)$$

$$\text{Frequency Domain Input Signal} \quad X(k) = \frac{Y(k)}{H(k)} \quad (34)$$

$$\text{Time Domain Conversion} \quad x(n) = IFFT(X(k)) \quad (35)$$

Recall Fig. 24 from chapter 4.3. Depending on whether the source or probe input is to be viewed depends on which transfer function is selected. Using $H1(s)$ allows viewing at the RFIC probe input. By selecting $H2(s)$, the voltage source is viewed. $H2(s)$ will enable viewing the input as if the probe does not load the node.

6.3 Colpitts Oscillator

Fig. 31 through Table 3 represents probing the Colpitts oscillator. $H1(s)$ is used to recreate V_{out} . Using the built in ADS functions; $H1(s)$ is calculated from the derived Z parameters. The FFT is represented as fs and the IFFT is represented as ts (Fig. 31). $H2(s)$ cannot predict the frequency shift and other adverse affects that putting a load on an oscillator so it is not used. Both probed and un-probed oscillators are compared for amplitude and apparent phase shift caused by a frequency shift (Fig. 32). Fig. 33 demonstrates circuit failure by loading a sensitive high impedance node too much. The input impedance of the probe will change the frequency of the oscillator tank circuit. Table 3 shows the frequency and power of the fundamental oscillation frequency to the 12 harmonic using a harmonic balance analysis in ADS. The probe shifted the oscillation frequency by 0.2%.

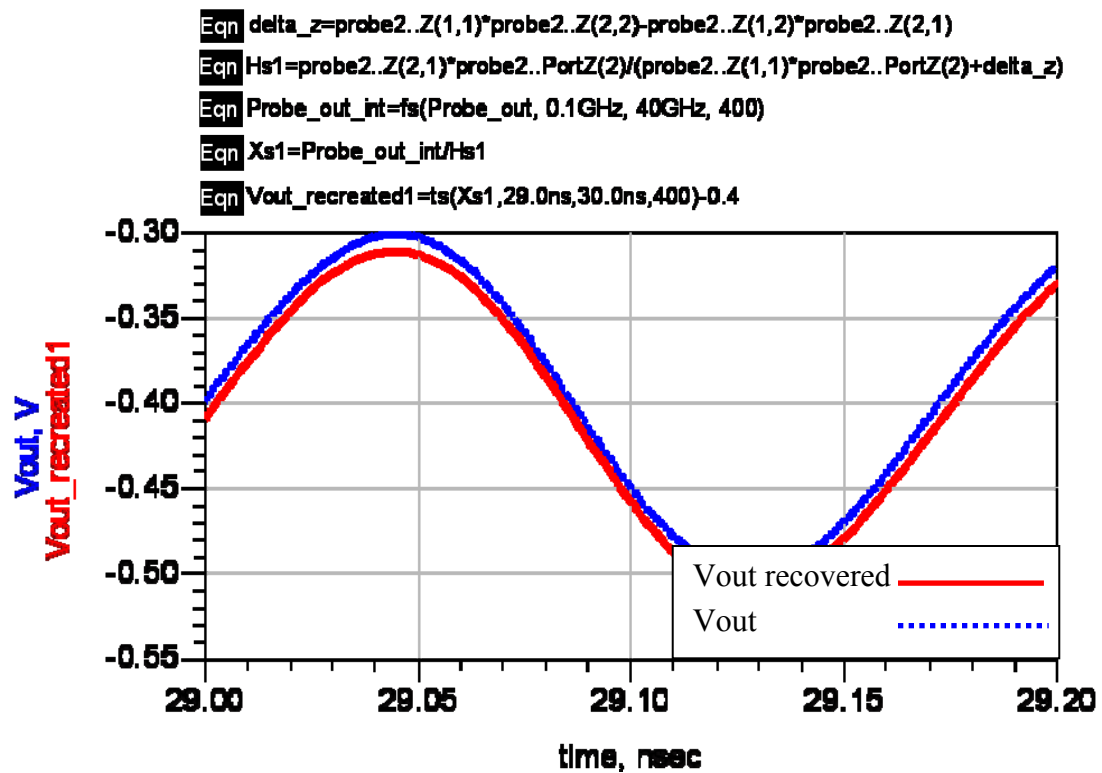


Fig. 31 Colpitts Oscillator Output.
Using $H1(s)$ the output signal is faithfully recreated.

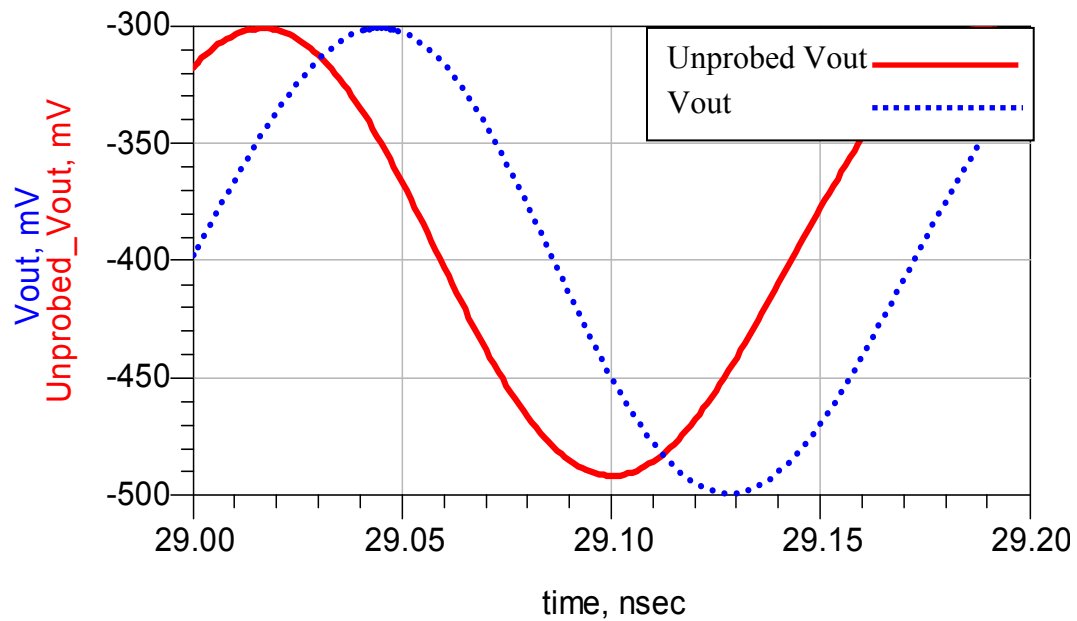


Fig. 32 Probed and Un-probed Circuits are Compared.
The probe loads the Colpitts oscillator output and causes a slight frequency change from the un-probed oscillator.

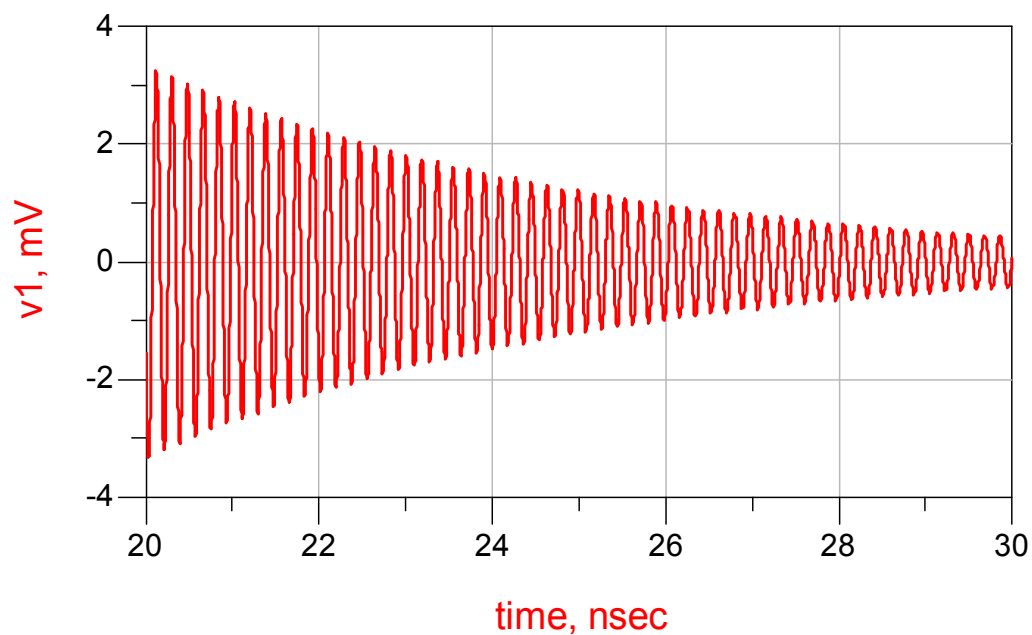


Fig. 33 Colpitts V1 Failure.
Probing the sensitive v_1 node causes oscillator failure.

Table 3
Colpitts Oscillator Spectral Analysis
Both probed and un-probed oscillators are compared to the 12th harmonic.

Harmonic	Probed_Colpitts		Unprobed_Colpitts	
Index	Freq. (GHz)	Spectrum	Freq. (GHz)	Spectrum
0	0.00	2.0	0.00	2.0
1	5.78	-10.1	5.79	-10.4
2	11.57	-40.7	11.58	-41.4
3	17.35	-58.0	17.37	-58.6
4	23.14	-65.5	23.16	-66.4
5	28.92	-74.3	28.95	-75.2
6	34.71	-79.0	34.75	-79.9
7	40.49	-83.6	40.54	-84.6
8	46.28	-90.0	46.33	-91.0
9	52.06	-89.9	52.12	-91.1
10	57.85	-102.7	57.91	-103.1
11	63.63	-95.7	63.70	-97.1
12	69.42	-114.1	69.49	-114.3

6.4 Cross Coupled Oscillator

Fig. 34 through Table 4 represent probing the Cross Coupled oscillator. H1(s) is used to recreate Vout. Using the built in ADS functions, H1(s) is calculated from the derived Z parameters. The FFT is represented as fs and the IFFT is represented as ts (Fig. 34). H2(s) cannot predict the frequency shift and other adverse affects that putting a load on an oscillator so it is not used. Both probed and un-probed oscillators are compared for amplitude and apparent phase shift caused by a frequency shift (Fig. 35). With a symmetric oscillator design as is the cross coupled, node v1 will give a response similar to Vout. Node V1 plots are not shown. The input impedance of the probe will change the frequency of the oscillator tank circuit. Table 4 shows the frequency and power of the fundamental oscillation frequency to the 12 harmonic using a harmonic balance analysis in ADS. The probe shifted the oscillation frequency by 2.4%.

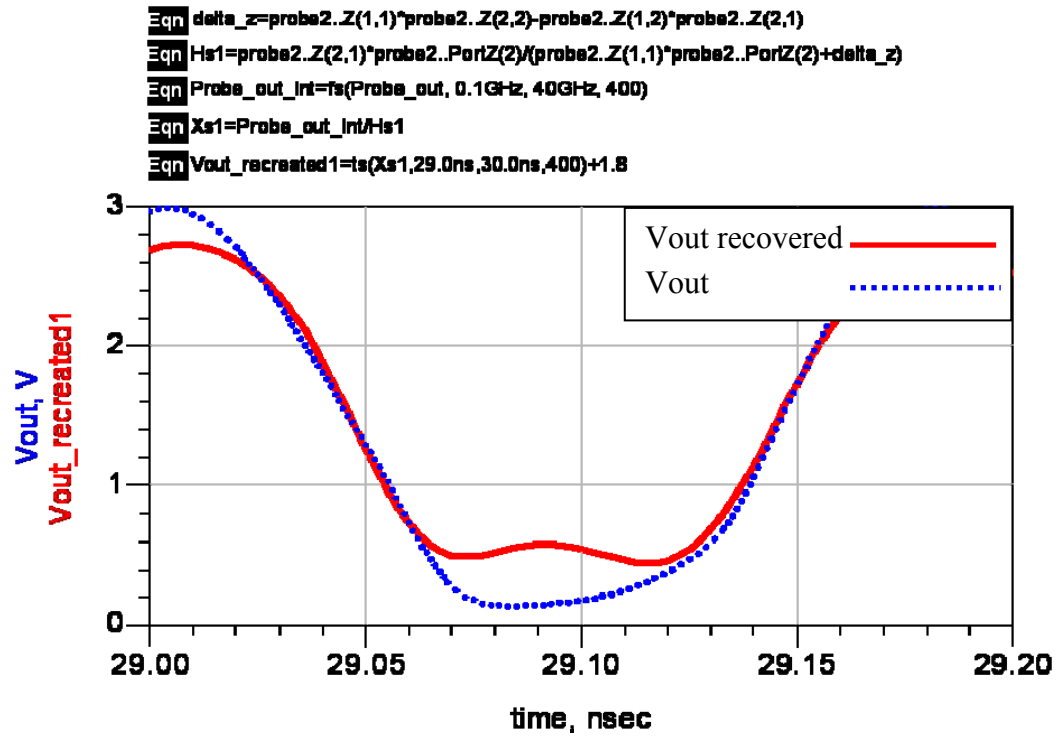


Fig. 34 Cross Coupled Oscillator Output.
Using H1(s) the output signal is faithfully recreated.

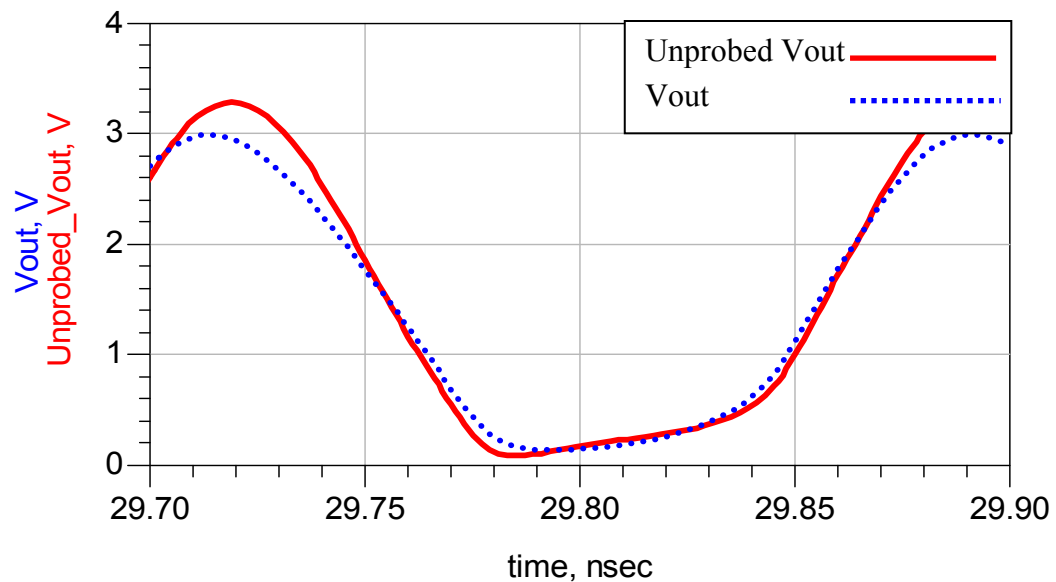


Fig. 35 Probed and Un-probed Circuits are Compared.
The probe loads the Colpitts oscillator output and causes a slight frequency change from the un-probed oscillator.

Table 4
Cross Coupled Oscillator Spectral Analysis
Both probed and un-probed oscillators are compared to the 12th harmonic.

Harmonic	Probed_Cross-Coupled		Unprobed_Cross-Coupled	
Index	Freq. (GHz)	Spectrum	Freq. (GHz)	Spectrum
0	0.00	12.7	0.00	12.8
1	5.67	13.4	5.81	14.1
2	11.34	-2.8	11.61	2.4
3	17.01	-10.4	17.42	-14.6
4	22.67	-27.3	23.22	-27.9
5	28.34	-24.5	29.03	-23.0
6	34.01	-27.1	34.83	-27.7
7	39.68	-39.0	40.64	-32.7
8	45.35	-30.9	46.44	-31.9
9	51.02	-43.6	52.25	-45.4
10	56.69	-43.3	58.05	-38.3
11	62.36	-57.5	63.86	-54.5
12	68.02	-53.6	69.66	-46.0

6.5 22nm Inverter

Fig. 36 through Fig. 38 represent probing a 22nm inverter running at 10GHz. Typically CMOS circuits are not forgiving to capacitive loads. Fig. 36 demonstrates using H1(s) to recreate Vout. Using the built in ADS functions, H1(s) is calculated from the derived Z parameters. The FFT is represented as fs and the IFFT is represented as ts. Fig. 37 demonstrates using H2(s) to derive Vout without the probe loading. ADS calculates H2(s) directly from S(2,1). Fig. 38 checks the next inverter stage to ensure that the signal is propagating through to that stage.

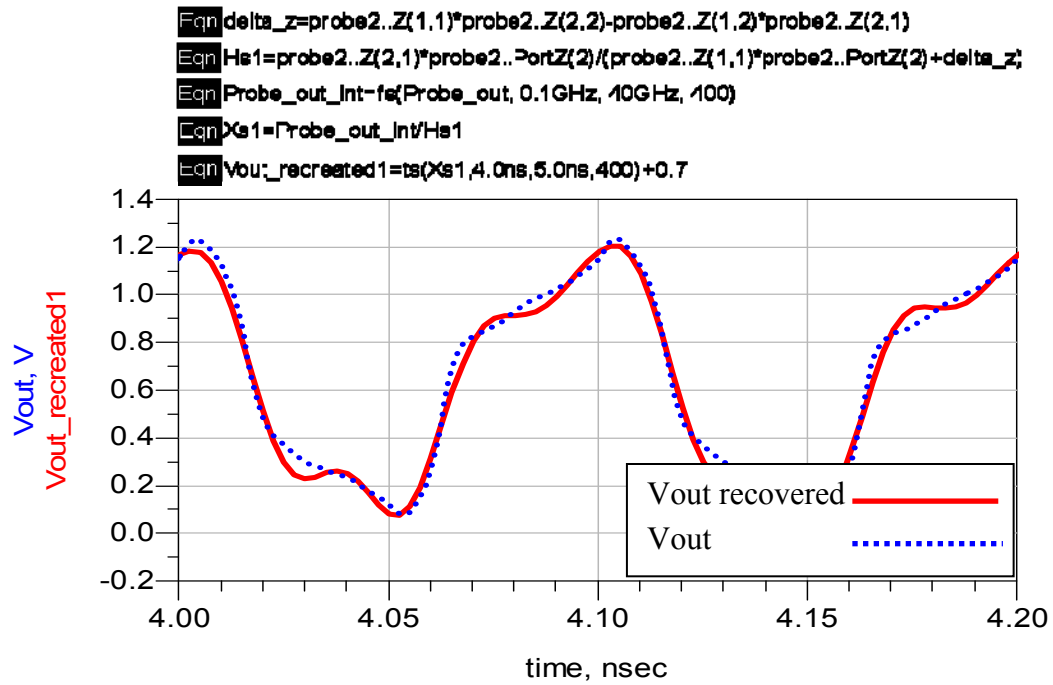


Fig. 36 H1(s) Representation of 22nm Inverter Running at 10GHz.
H1(s) the loaded output signal is faithfully recreated.

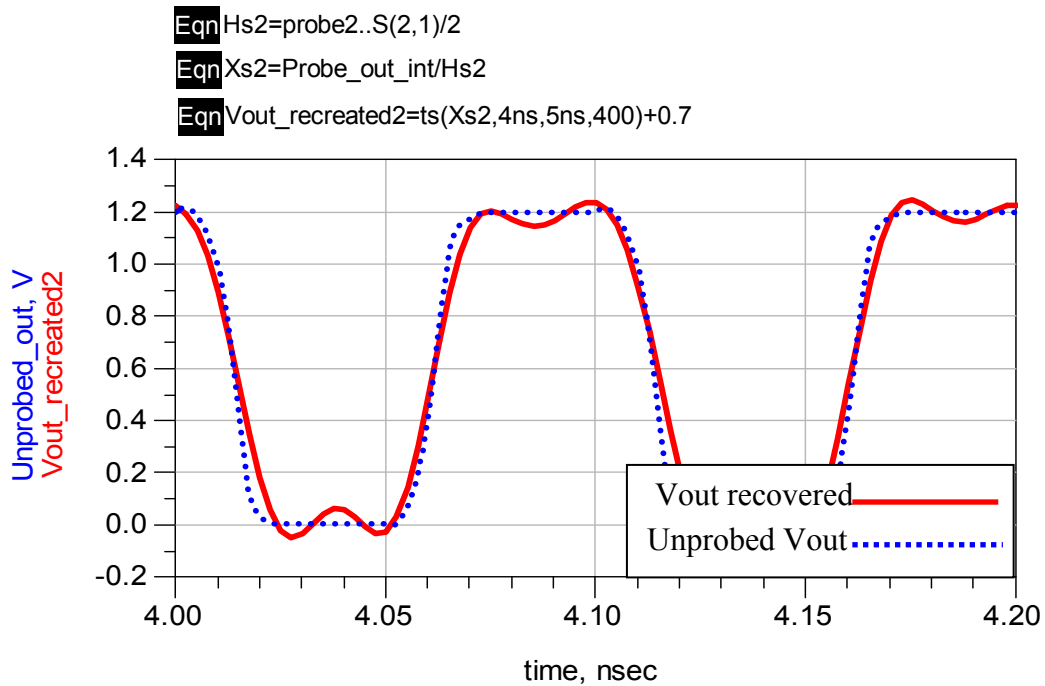


Fig. 37 H2(s) Representation of 22nm Inverter Running at 10GHz.
Using H2(s) the source signal is faithfully recreated. The signal appears as if the probe does not load the inverter.

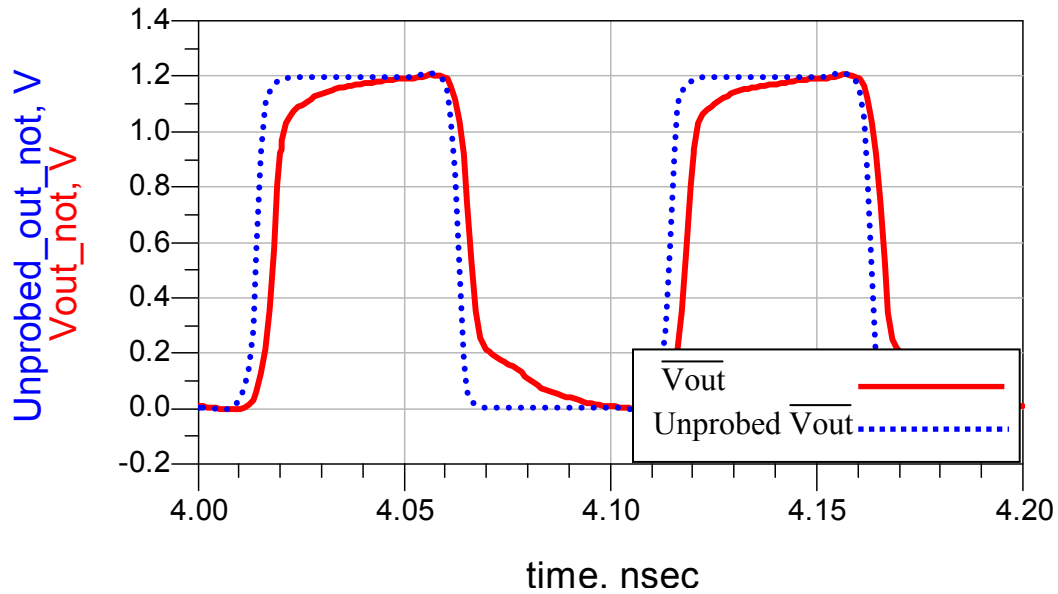


Fig. 38 Output of the Second Inverter.

The output of the next stage is illustrated for both a probed and un-probed inverter.

6.6 Measured Pulse Generator Signal

In the last sections, the extracted parameters from a manufactured probe are used on a simulated circuit. In this section, the manufactured probe is used on a real circuit.

A step waveform from a 200ps rise time pulse generator is terminated into 50 Ohms. The probe output of a high speed pulse generator is sampled with a high speed oscilloscope (Fig. 39). The pulse generator signal is also sampled and displayed using a microwave probe along with the recovered input signal from the RFIC probe (Fig. 40). As in the simulations, the RFIC probe transfer function is determined and the step output of the high speed pulse generator is recovered using the Matlab FFT and IFFT functions.

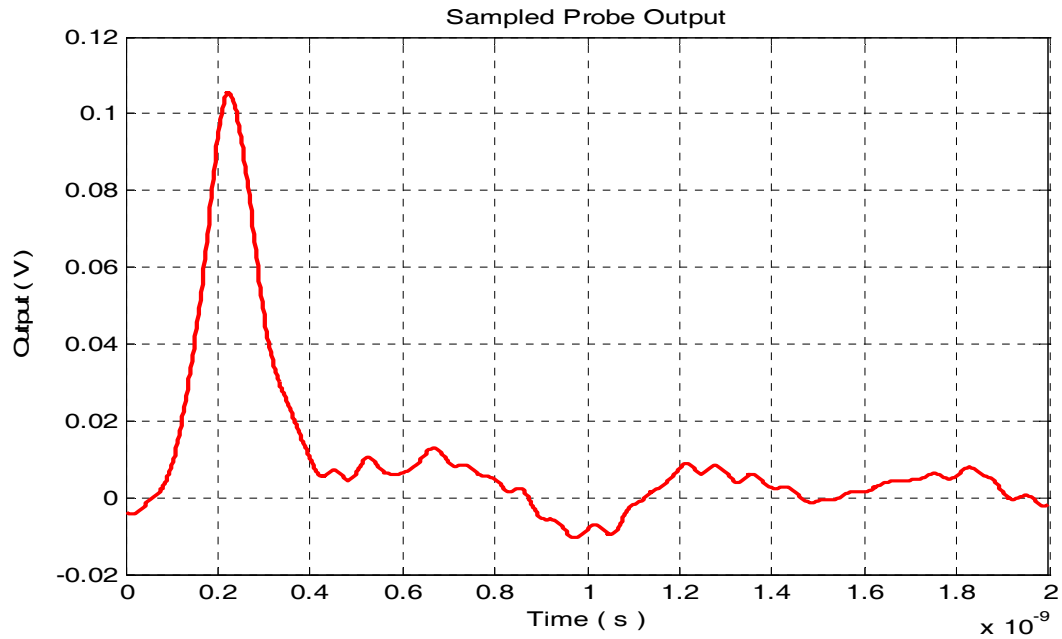


Fig. 39 Sampled Probe Output

The probe signal is displayed using a 50 G samples per second oscilloscope

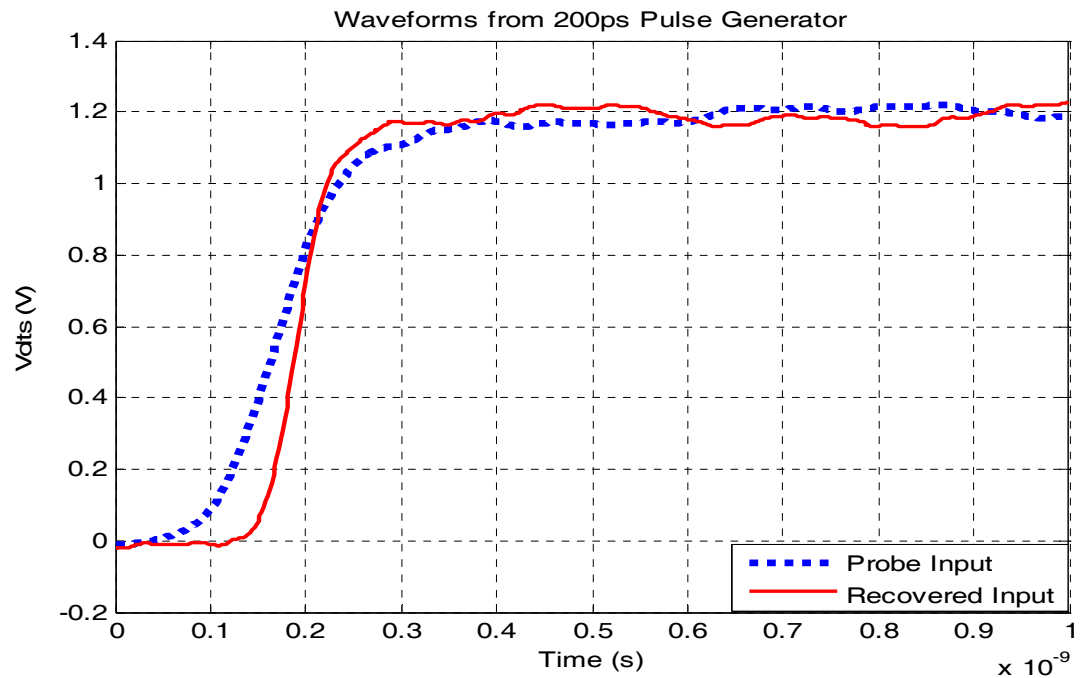


Fig. 40 Pulse Generator Waveform and the Recovered Signal

A 200ps risetime signal is displayed on a 50G sample/second oscilloscope using a microwave probe. The recovered signal from the RFIC probe is calculated and displayed concurrently.

7 CONCLUSION

The RFIC probe presented in this work demonstrates that high impedance circuits operating at high frequency can be successfully probed. The probe has an ultra low 30fF input capacitance to minimize circuit loading. 30fF is the lowest input capacitance of available high impedance probes. Knowing the impedance of the DUT, both V_{in} (loaded) and V_s (unloaded) waveforms can be recovered by selecting the appropriate transfer function, $S1(s)$ or $S2(s)$.

The probe has a slim streamline design enabling better circuit viewing in a probe station. Mechanically, the probe is easy to manufacture. Depending on the application required, loading impedance and resonance frequency can be adjusted by altering construction dimensions.

Future work may include adding resistance to the probe needle. This will lower the probe Q. Resonance and anti-resonance points will be softened, leading to a more consistent loading impedance above 15GHz. Characterizing the RFIC probe to 40GHz limits the probe frequency response. Characterizing the probe to a higher frequency will extend its frequency response. Moving the software component of the RFIC probe into a sampling oscilloscope will enable almost real time viewing of the recovered signal.

BIBLIOGRAPHY

- [1] B. D. Beste and S. Griffiths. (2002, Oct.) Bill & Stan's Tektronix Resource Site. [Online].
http://www.reprise.com/host/tektronix/reference/voltage_probes.asp
- [2] Z. Yang, L. Wojewoda, L. Smith, H. Ishida, and M. Shimizu, "Inductance of Bypass Capacitors," in *DesignCon 2005*, Santa Clara, 2005, pp. 1-52.
- [3] Tektronix. (2009, Feb.) Tektronix Enabling Innovation. [Online].
http://www.tek.com/products/accessories/oscilloscope_probes/
- [4] American Probe & Technologies, Inc. (2005, Jan.) American Probe & Technologies, Inc. Home of the finest probing accessories. [Online].
<http://www.americanprobe.com/triaxial-ph.htm>
- [5] Cascade Microtech, Inc. (2009, Feb.) Cascade Microtech, Inc. [Online].
<http://www.cmicro.com/products/engineering-probes/rf-microwave>
- [6] GGB Industries Inc. Picoprobe. [Online]. <http://www.ggb.com/index.html>
- [7] W. S. Coates, R. J. Bosnyak, and I. E. Sutherland, "Method and apparatus for probing an integrated circuit through capacitive coupling," Capacitively-coupled test probe Patent 6600325, Jul. 29, 2003.
- [8] D. T. Crook and e. al, "Capacitively-coupled test probe," U.S. Patent 5274336, Dec. 28, 1993.
- [9] G. E. Bridges, " Non-contact probing of integrated circuits and packages," *Microwave Symposium Digest, 2004 IEEE MTT-S International*, pp. 1805-1808, Jun. 2004.
- [10] M. Tech. (2008, Dec.) Applied Chemical and Morphological Analysis Laboratory. [Online]. <http://mcff.mtu.edu/acmal/veecodim3000.htm>
- [11] G. Majidi-Ahy and D. M. Bloom, "Millimeter-wave active probe system," U.S. Patent 5003253, Mar. 3, 1989.
- [12] W. D. Edwards, J. G. Smith, and H. A. Kemhadjian, "SOME INVESTIGATIONS INTO OPTICAL PROBE TESTING OF INTEGRATED CIRCUITS.," *Radio and Electronic Engineer*, vol. 46, no. 1, p. 35, 1976.
- [13] Agilent Technologies Inc. (2009) Manuals: Oscilloscope probes and accessories.
- [14] D. M. Lauterbach, "Oscilloscope active probe," *Test & Measurement World*, Aug. 2001.

BIBLIOGRAPHY (Continued)

- [15] R. J. Adler. (2007) North Star High Voltage. [Online].
<http://www.highvoltageprobes.com/index.html>
- [16] S. M. Goldwater. (2009, Mar.) High Voltage Probe Frequency Response. [Online]. <http://www.repairfaq.org/sam/hvprobe.htm#shvmhf>
- [17] J. L. Saunders and A. R. Loudermilk, "Methods for making contact device for making connection to an electronic circuit device and methods of using the same," USA Patent 6343369 B1, Jan. 29, 2002.
- [18] G. E. Bridges, "Non-contact probing of integrated circuits and packages," in *Microwave Symposium*, Fort Worth, TX, 2004, pp. 1805-1808.
- [19] F Ho, A. S. Hou, B. A. Nechay, D. M. Bloom, "Ultrafast voltage-contrast scanning probe microscopy," *Nanotechnology*, pp. 385-389, 1996.
- [20] Z. Weng, T. Kaminski, G. E. Bridges, and D. J. Thomson, "Resolution enhancement in probing of high-speed integrated circuits using dynamic electrostatic force-gradient microscopy," *Journal of Vacuum Science and Technology A*, pp. 948-953, 2004.
- [21] C. J. Falkingham, I. H. Edwards, and G. E. Bridges, "Non-contact internal-MMIC measurement using scanning force probing," in *Proceedings of the 1999 IEEE MTT-S International Microwave Symposium*, Boston, MA, 2000, pp. 1619-1622.
- [22] W. Mertin, "Contactless probing of high-frequency electrical signals with scanning probe microscopy," in *IEEE MTT-S International Microwave Symposium Digest*, Seattle, WA, 2002, pp. 1493-1496.
- [23] K. R. Gleason and K. E. Jones, "High-frequency active probe having replaceable contact needles," U.S. Patent 5045781, Sep. 3, 1991.
- [24] T. J. Zamborelli, "Wide bandwidth passive probe," U.S. Patent 5172051, Dec. 15, 1992.
- [25] K. Yang, G. David, and S. W. J. F. Robertson, "High-resolution electro-optic mapping of near-field distributions in integrated microwave circuits," in *Microwave Symposium*, Baltimore, MD, 1998, pp. 949-952.
- [26] D.-J. Lee and J. F. Whitaker, "An optical-fiber-scale electro-optic probe for minimally invasive high-frequency field sensing," *Optics Express*, vol. 16, no. 26, pp. 21587-21597, Dec. 2008.
- [27] A. Weisshaar, *ECE 699 class notes*. Corvallis, Oregon, Dept of EECS, Oregon State University, Fall 2007.

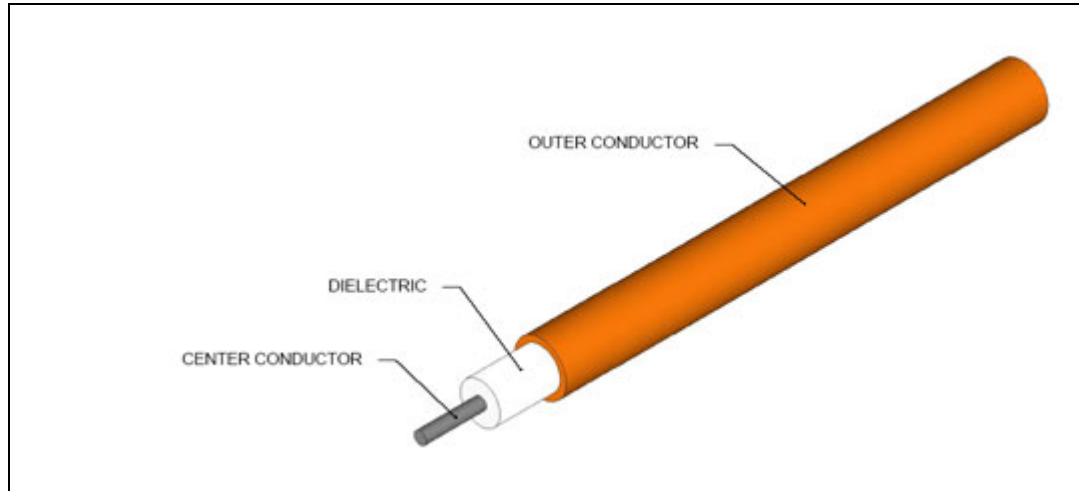
BIBLIOGRAPHY (Continued)

- [28] L. Forbes, D. A. Miller, and M. E. Jacob, "Low capacitance electrical probe for nanoscale devices and circuits," *Open Nanoscience Journal*, vol. 2, no. 1, pp. 39-43, Aug. 2008.
- [29] Micro-Coax, *UT-47-M17 Data Sheet*. 2003, Cut-off frequency is 136GHz.
- [30] J. W. Nilsson and S. A. Riedel, *Electric Circuits, 6th ed.* Upper Saddle River, New Jersey, USA: Prentice-Hall, 2000.
- [31] Micro-Coax. (2003) Micro-Coax. [Online]. <http://www.micro-coax.com/pages/technicalinfo/applications/26.asp>
- [32] P-N Designs Inc. (2006, Apr.) Microwaves101.com. [Online]. <http://www.microwaves101.com/encyclopedia/connectorsprecision.cfm#24mm>
- [33] B. Frank. (2007, Sep.) Queen's University. [Online]. http://bmf.ece.queensu.ca/mediawiki/index.php/Network_Parameters
- [34] K. Mayaram, *ECE 621 class notes*. Corvallis, Oregon: Dept of EECS, Oregon State University, Winter 2008.
- [35] T. N. Cokienias, "New rules for unlicensed digital transmission systems," *Compliance Engineering*, no. Spring, 2002.
- [36] Nanoscale Integration and Modeling (NIMO) Group,. (2007, Oct.) Predictive Technology Model (PTM). [Online]. <http://www.eas.asu.edu/~ptm/latest.html>
- [37] S. Haykin and B. V. Veen, *Signals and Systems Second Edition*, B. Zobrist, Ed. Hoboken, United States of America: John Wiley & Sons Inc., 2003.
- [38] M. E. Jacob, D. A. Miller, and L. Forbes, "Ultra low capacitance high frequency IC probe," *Proceedings of SPIE, the International Society for Optical Engineering*, vol. 7042, pp. 7042031-7042039, Aug. 2008.
- [39] M. E. Jacob, D. A. Miller, and L. Forbes, "Ultra low capacitance, high frequency RFIC probe," in *2008 IEEE Workshop on Microelectronics and Electron Devices (WMED)*, Boise, 2008, pp. 32-33.

APPENDICES

Appendix A – Coaxial Specifications

MICRO-COAX[®] <i>Leading the way in transmission line solutions.</i>		UT-47-M17 (M17/151-00001)	
206 Jones Blvd. Pottstown, PA 19464 USA Phone: 610-495-0110 : 800-223-2629 www.micro-coax.com		Semi-Rigid Coaxial Cable	
MECHANICAL CHARACTERISTICS			
Outer Conductor Diameter, inch (mm)	0.047+/-0.001 (1.194+/-0.0254)		
Dielectric Diameter, inch (mm)	0.037 (0.94)		
Center Conductor Diameter, inch (mm)	0.0113+/-0.0005 (0.287+/-0.0127)		
Maximum Length, feet (meters)	20 (6.1)		
Minimum Inside Bend Radius, inch (mm)	0.125 (3.175)		
Weight, pounds/100 ft. (kg/100 meters)	0.45 (0.67)		
ELECTRICAL CHARACTERISTICS			
Impedance, ohms	50+/-2.5		
Frequency Range GHz	DC-20		
Velocity of Propagation %	70		
Capacitance, pF/ft. (pF/meter)	32.2 (105.6)		
Typical Insertion Loss, dB/ft. (dB/meter)	Frequency	Insertion Loss	Power
and Average Power Handling, Watts CW at 20 degrees Celsius and Sea level	0.5 GHz	0.28 (0.92)	45
	1.0 GHz	0.40 (1.31)	32
	5.0 GHz	0.90 (2.95)	13
	10.0 GHz	1.30 (4.27)	9
	20.0 GHz	1.90 (6.23)	6.5
Corona Extinction Voltage, VRMS @ 60 Hz	1000		
Voltage Withstand, VRMS @ 60 Hz	2000		
ENVIRONMENTAL CHARACTERISTICS			
Outer Conductor Integrity Temperature, Deg Celsius	175		
Maximum Operating Temperature, Deg Celsius	100		
MATERIALS			
Outer Conductor	Copper		
Dielectric	PTFE		
Center Conductor	SPCW		
CUTAWAY			



MICRO-COAX®
 Leading the way in transmission line solutions.

206 Jones Blvd. Pottstown, PA 19464 USA
 Phone: 610-495-0110 : 800-223-2629
www.micro-coax.com

Attenuation (Theoretical) at 20°C

$$\alpha = \frac{0.434}{Z_0} \left(\frac{\sqrt{R_1}}{d} + \frac{\sqrt{R_2}}{D} \right) + 2.78 F \sqrt{e} P_f \quad \dots \text{dB/100 ft}$$

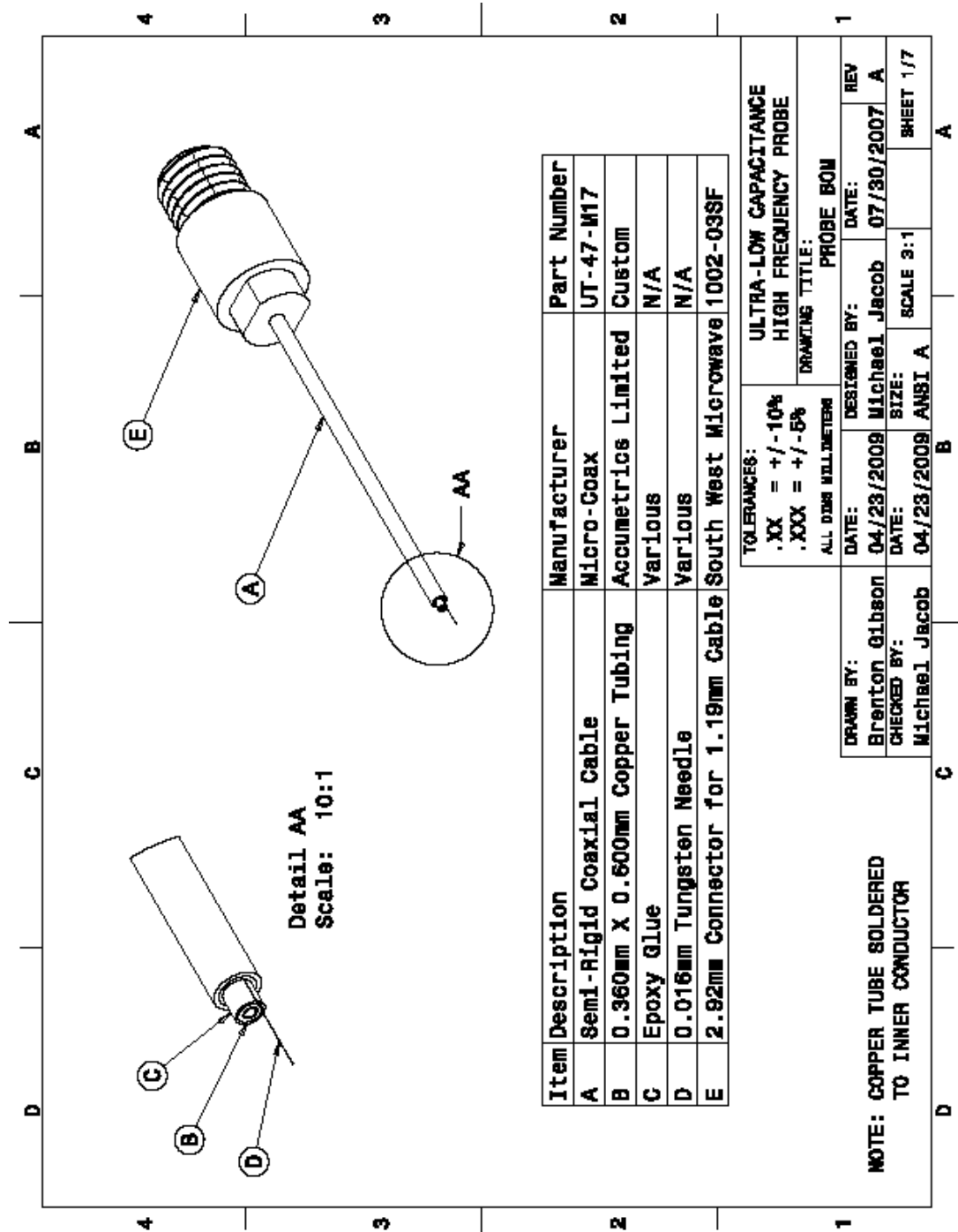
α	Attenuation
Z_0	Characteristic impedance
R_1	Ratio of center conductor conductivity to copper (usually =1 for SPC or SPCW conductors)
R_2	Ratio of outer conductor conductivity to copper (usually =1 for SPC or SPCW conductors)
D	Dielectric diameter, inches
d	Center conductor diameter, inches
e	Dielectric constant
F	Frequency in MHz
P_f	Dielectric Power factor (0.0002 for solid or spline PTFE, 0.000064 for LL or ULL PTFE)

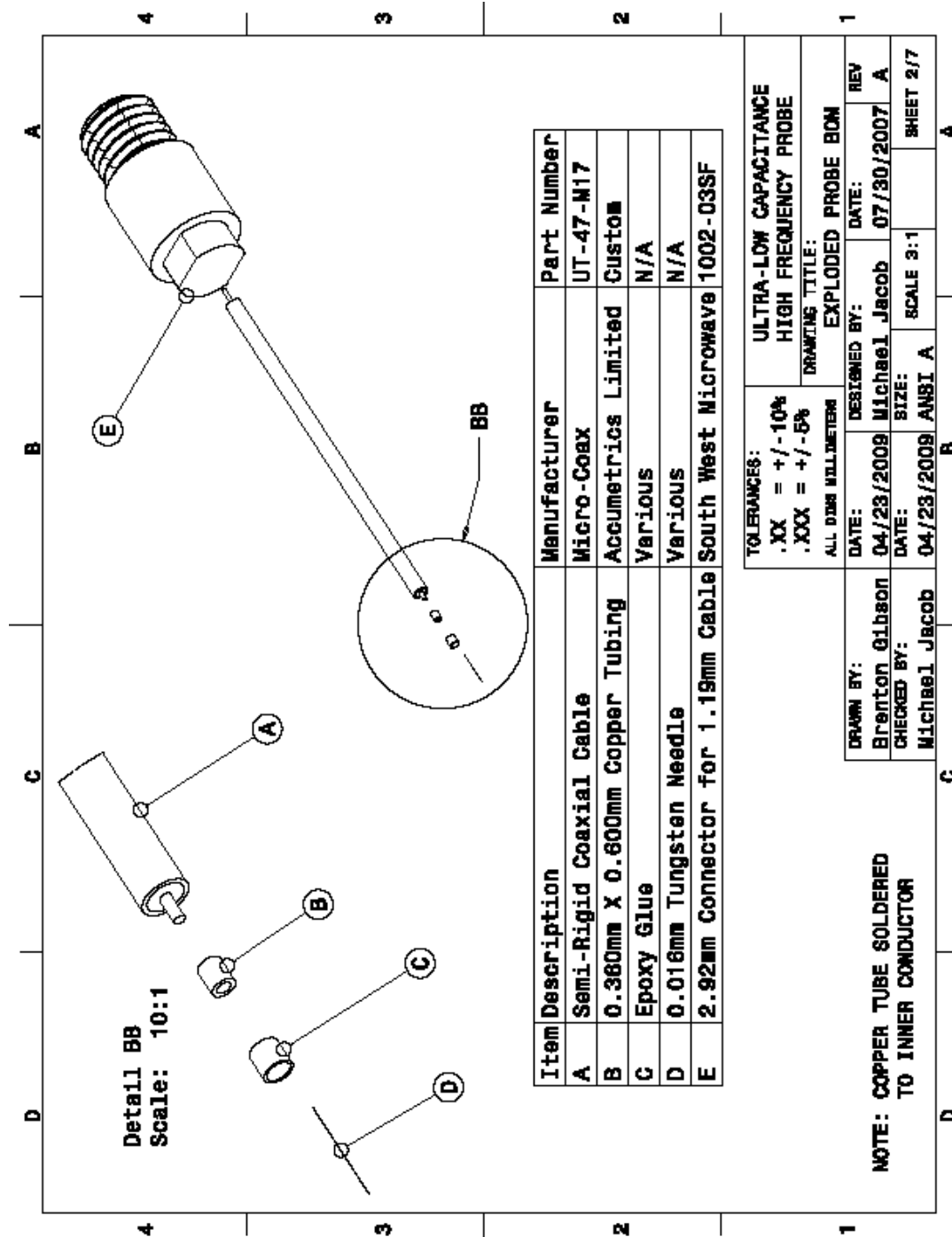
Cutoff Frequency

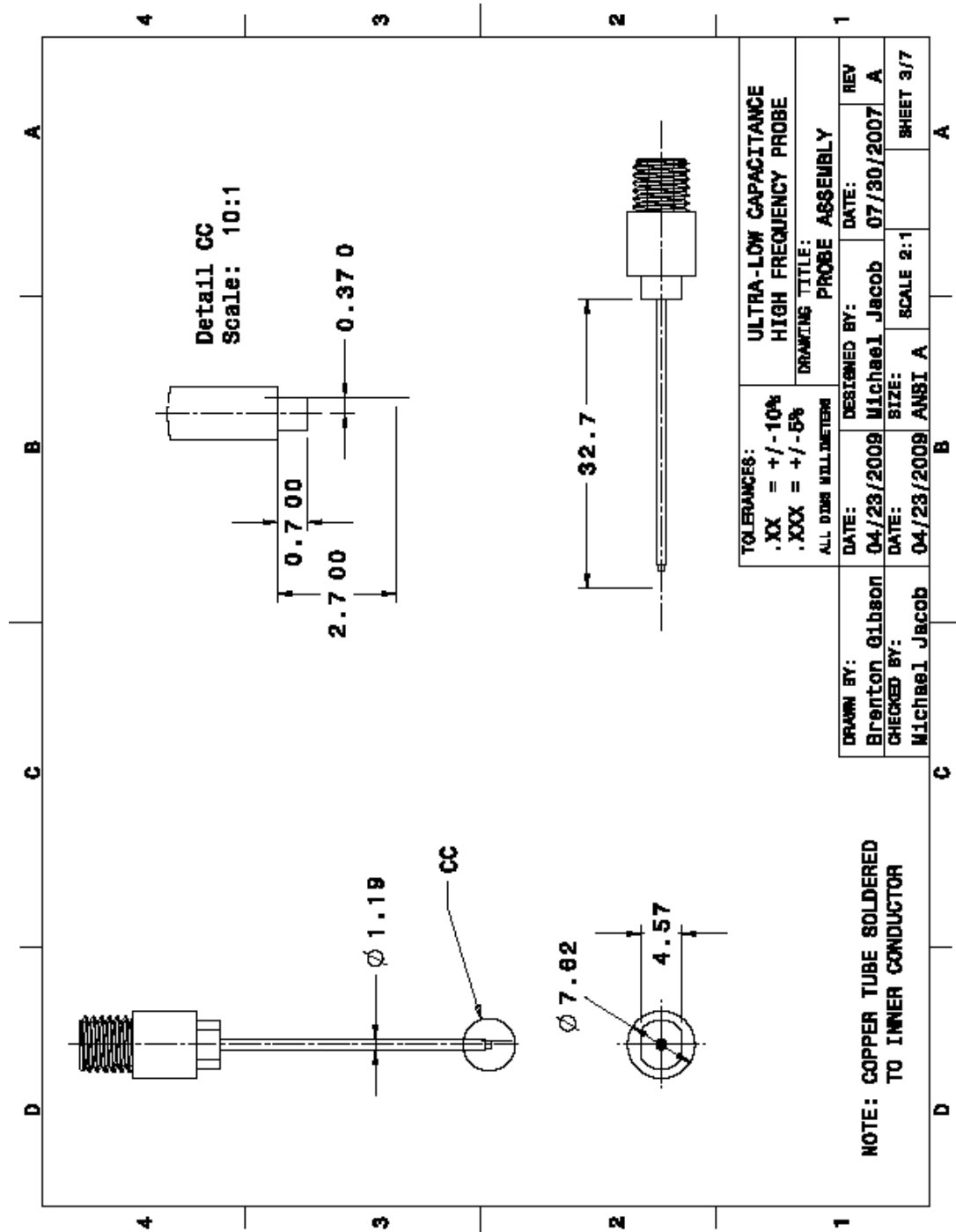
$$F_{co} = \frac{7.5}{\sqrt{e} (D + d)} \quad \dots \text{GHz}$$

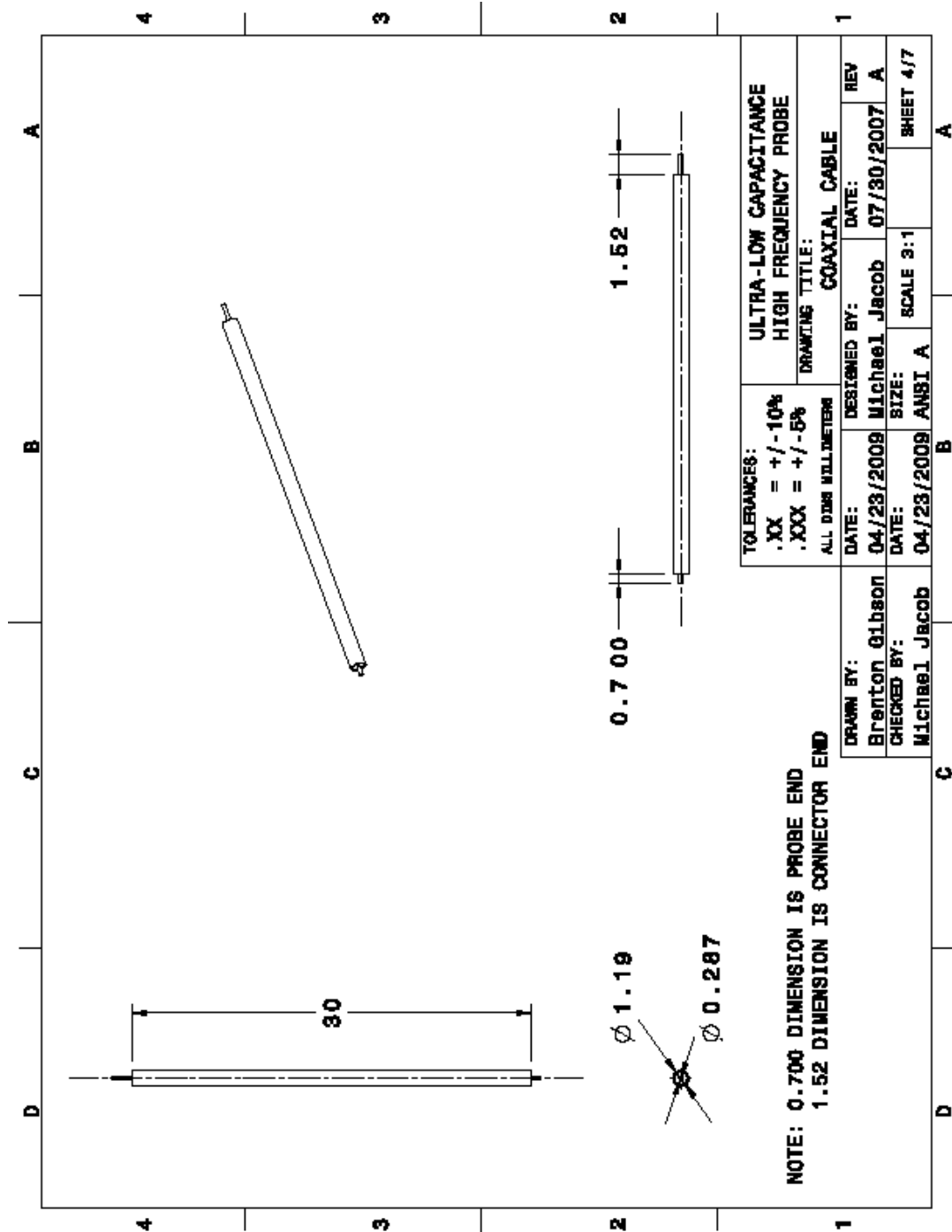
e	Dielectric constant
D	Dielectric diameter, inches
d	Center conductor diameter, inches

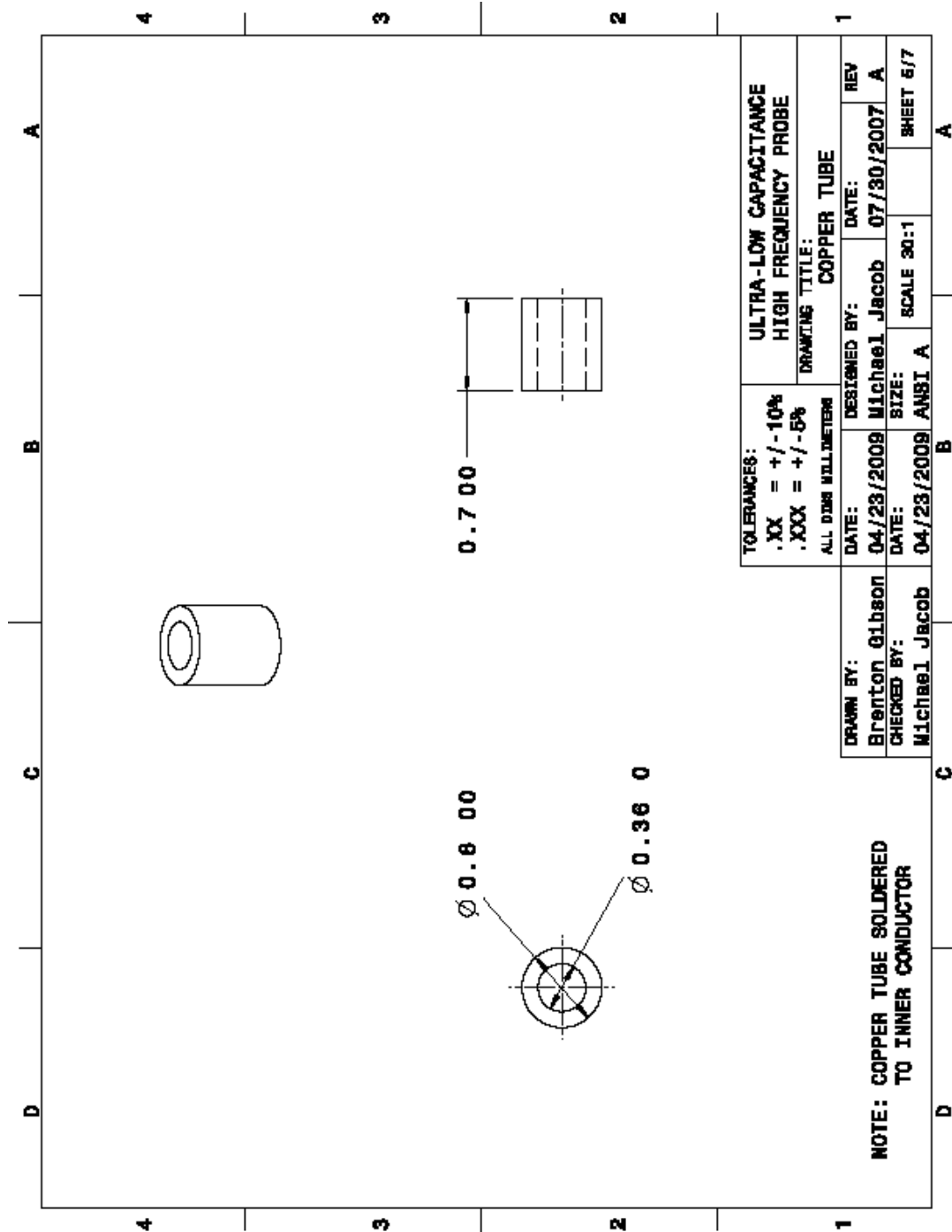
Appendix B – Probe Design

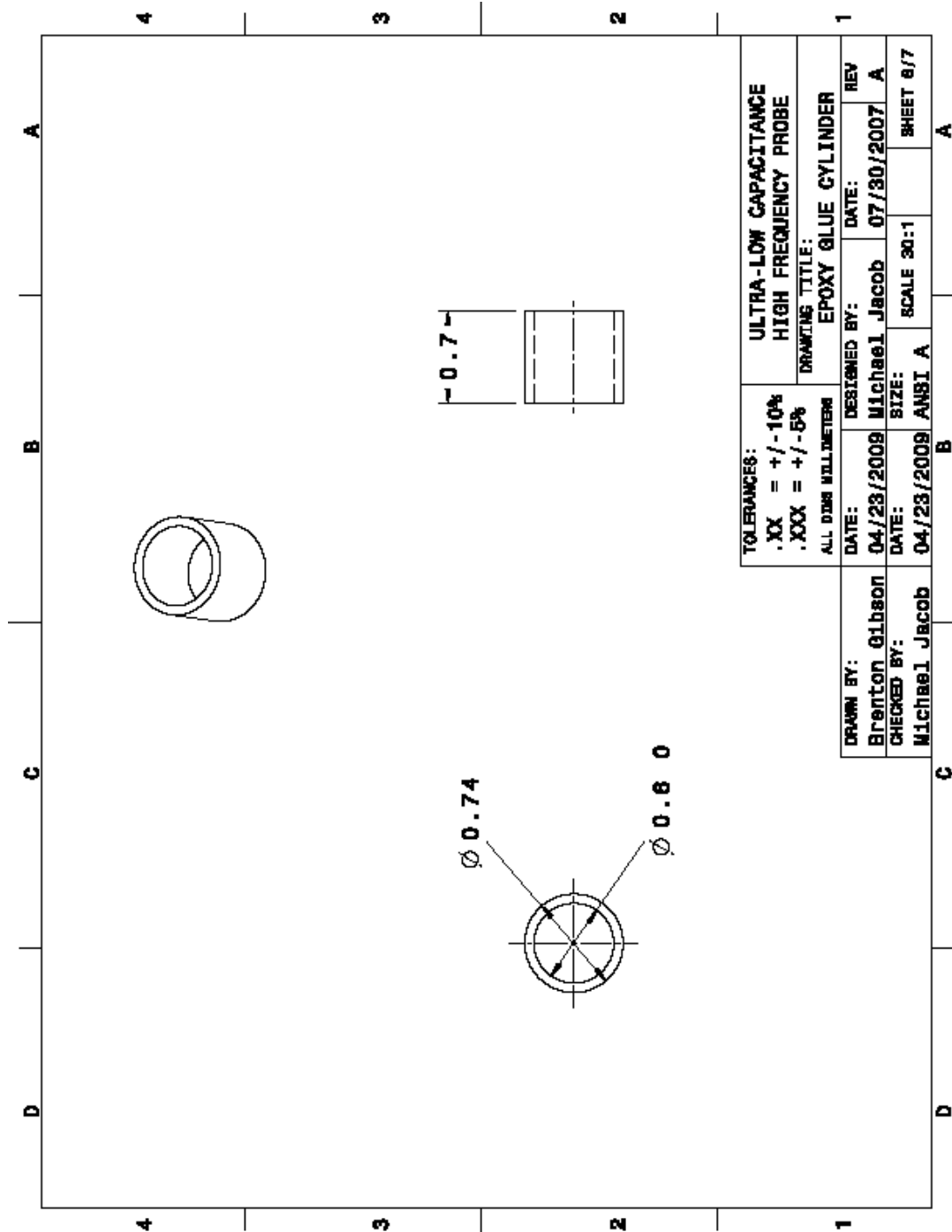


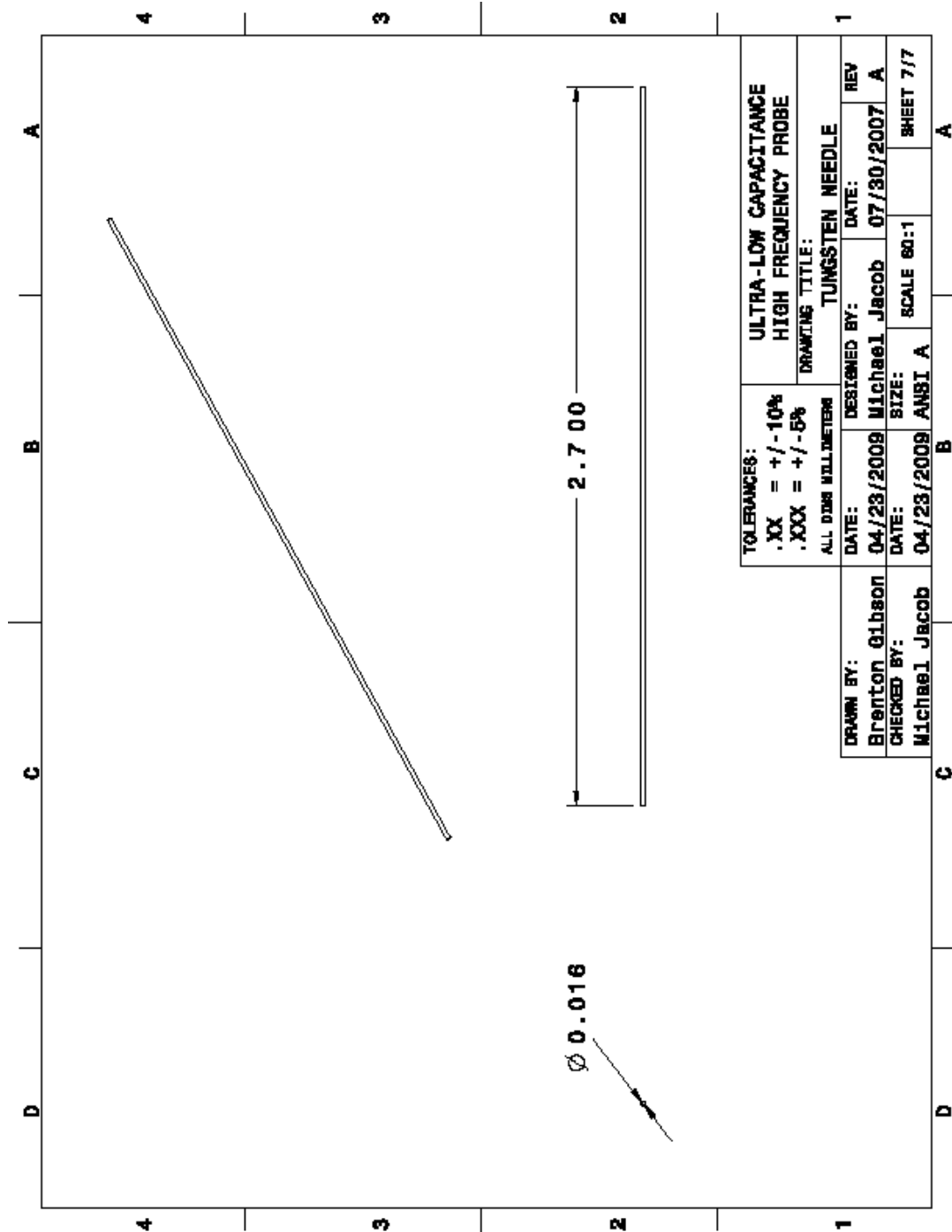












TOLERANCES:		ULTRA-LOW CAPACITANCE	
.XX = +/-10%		HIGH FREQUENCY PROBE	
.XXX = +/-5%		DRAWING TITLE:	
ALL DIMS IN MILLIMETERS		TUNGSTEN NEEDLE	
DRAWN BY:	DESIGNED BY:	DATE:	REV
Brenton Gibson	Michael Jacob	07/30/2007	A
CHECKED BY:	SIZE:	SCALE	SHEET 7/7
Michael Jacob	ANSI A	80:1	

Appendix C – Test Substrate

Impedance Standard Substrate

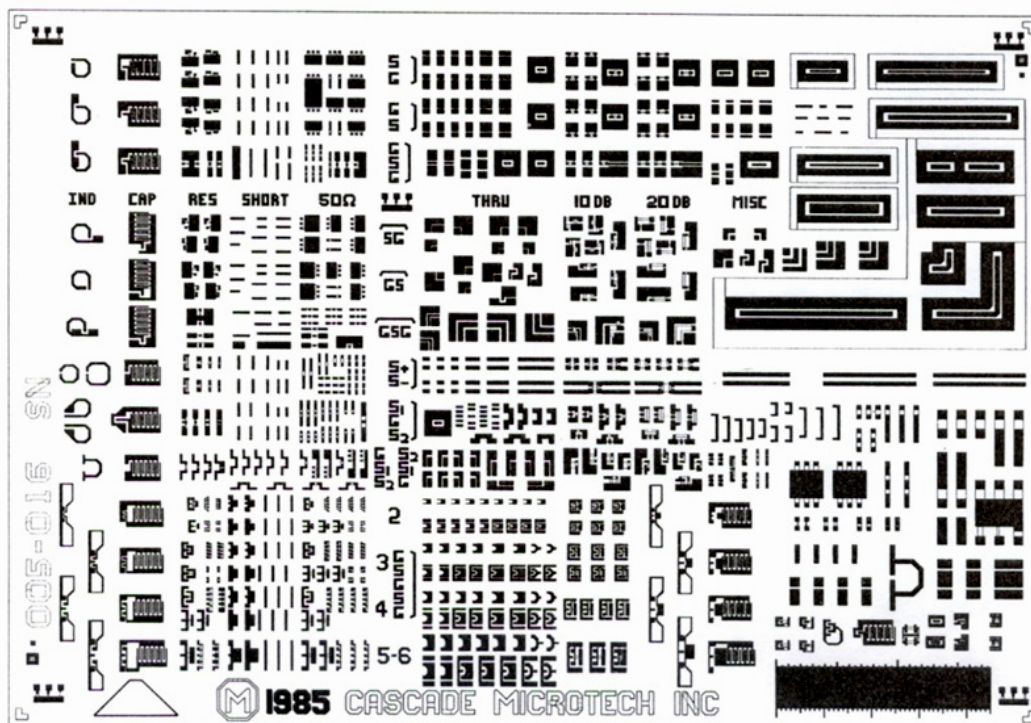


Fig. 4-19 Text reference is to 1985
ISS version (PN 005-016)

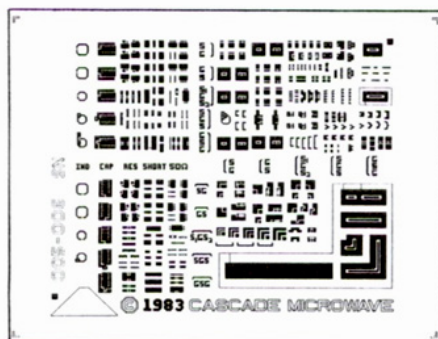


Fig. 4-20 1983 ISS version

Introduction Cascade Microtech microwave probe heads (acting as adapters from coaxial cable to the impedance standard substrate elements) make contact to the impedance standard substrate (ISS) short circuits, load standards, and through-connection standards during the calibration process. The open circuit is created by lifting the probe(s) at least 10 mils (0.25 mm) into the air. This calibration process is similar to using coaxial impedance standards.

The impedance standard substrate (ISS) has calibration and verification standards for all standard probe heads, in most configurations. The standards are useful for making corrected and uncorrected microwave measurements.

One-port inductor, capacitor, load verification, short-circuit, and 50 ohm load standards are located on the ISS left side. Two-port standards are on the right side.

Appendix D – HSpice, 2D Circuit Simulation

```

*****
* Whisker_coupler_together7.23.sp
* Author: Drake Miller & Michael Jacob
* Date: 7/16/07
* Revised 7.23.07 Michael Jacob
* W element field solver for probe whisker attached to coupler
*****

*****
*Constants
*****
.PARAM      Whs_len      =      "2mm"
.PARAM      coup_len     =      "0.7mm"
.PARAM      CtoC_sep     =      "0.185mm"
.PARAM      whs_rad      =      "8um"

.PARAM      coax_inner_rad =      "100um"
.PARAM layer_pos          =      "2.5mm+CtoC_sep"
.OPTION PROBE POST
*****

*2ps rise time pulse
*****
VIMPULSE 1 gnd PULSE 0v 1v 5p 2p 2p 50p      *use for tran
*i1      1      gnd AC 1                      *use for AC

*****
*U Element simulates whisker
*The 3mm Tungsten Whisker by radius 10um
*****
U1 w_in gnd w_in1 gnd air_coax l="whs_len"      *Whisker length
Rinput  1 w_in      300                        *assume perfect input
R_con   w_in1 in1    0.01                      *connect whisker to coupler

*****
*W Element
*****
W1 in1 in2 gnd out1 out2 gnd
+ FSmodel=whisker N=2 l="coup_len"              *coupler overlap

Rin1    1 in1 .0325                             * least reflection at 325 ohms
Rin2   in2 gnd 325Meg                             * least reflection at 325 ohms
Rout2 out2 gnd 270                               *assume termination to ideal coax

*****
*Materials FR4 at 1 GHz
*****
.MATERIAL diel_fr4 DIELECTRIC ER=4.3 LOSSTANGENT=0.015
.MATERIAL diel_epoxy DIELECTRIC ER=4 LOSSTANGENT=0.015

```



```

.MATERIAL copper METAL CONDUCTIVITY=59.61meg

*****
* Coax Shapes
*****
.SHAPE whisker CIRCLE radius="whs_rad"           *whisker radius
.SHAPE micro_coax CIRCLE radius = "coax_inner_rad" *coax inner conductor radius

*****
*Uses the default AIR
*background
*****
.LAYERSTACK stack_1 LAYER=(PEC, 1um) + LAYER=(air,2.5mm) +
LAYER=(diel_epoxy,1mm)

*****
*Option settings
*****
.FSOPTIONS opt1 PRINTDATA=YES ACCURACY=HIGH

*****
*Two different conductor shapes
*Air coax
*****
.MODEL whisker W MODELTYPE=FieldSolver,
+ LAYERSTACK=stack_1, FSOPTIONS=opt1,
+ RLGCFILE=coupled.rlgc
+ CONDUCTOR=(SHAPE=whisker,ORIGIN=
+ (2.5mm, 5mm), MATERIAL=copper)
+ CONDUCTOR=(SHAPE=micro_coax,
+ ORIGIN=("layer_pos", 5mm), MATERIAL=copper)      *layer_pos is specified C to C plus
2.5mm

.MODEL air_coax u LEVEL=3 plev=2 elev=1
+ RA="whs_rad" RB=2.5mm RHO=52.9n RHOB=17n KD=1

*****
*Analysis, outputs and end
*****
.TRAN .1p 0.16n                                     *use for tran
*.tf v(out2) V(1)                                     *use for tran
*.AC Dec 1000 4GHz 40GHz                             *use for AC
.PROBE v(out2) v(in1) V(1) V(w_in) i(Rin1) i(Rw)      *probe V(w_in) whisker input impedance
*.PRINT v(1) v(w_in)                                *use for AC
.END

```

```

*****
* Whisker_coupler_coax_filter_simple_PWL_rev1.sp
* Author: Michael Jacob & Drake Miller
* Date: 7/25/07 Revised 7.30.07
* 8.21.07 add resistance and capacitance to DUT
* W element field solver for probe whisker attached to coupler, coax and filter
*
*****

*****
*Constants
*****
.PARAM      Whs_len      =      "2mm"
.PARAM      coup_len     =      "0.7mm"
.PARAM      CtoC_sep     =      "0.368mm"
.PARAM      whs_rad      =      "8um"
.PARAM      coax_inner_rad =      "0.3mm"
.PARAM layer_pos        =      "2.5mm+CtoC_sep"
*****
*2ps rise time pulse
*****
*VIMPULSE 1 gnd PULSE 0v 1v 0p 25p 75p 511p *use for tran
Vinpwl 1 gnd PWL (0ps, 0V) (20ps, 0V) (40ps, 1V) (60ps, 1V) (70ps, 2v) (80ps, 1V) (90ps,
2V) (100ps, 1V) (110ps, 2V) (120ps, 1V) (200ps, 1V) (300ps, 0.5v) (500ps, 0V)
*i1      1      gnd AC 1      *use for AC
Rinput  1 2      1000      *assume perfect input with 343 Ohms
Cinput  2 gnd      50fF      *assume 50fF parasitic cap
R_con1  2 w_in      0.01      *connects probe to circuit pick this or
*E1 w_in gnd 2 gnd 1      *isolates probe loading pick this

*****
*U Element simulates whisker
*The 3mm Tungsten Whisker by radius 10um
*****
U1 w_in gnd w_in1 gnd air_coax l="whs_len"      *Whisker length
R_con w_in1 in1      0.01      *connect whisker to coupler (should be zero)

*****
*W Element
*****
W1 in1 in2 gnd out1 out2 gnd
+ FModel=whisker N=2 l="coup_len"      *coupler overlap

Rin1 in2 gnd 325Meg      * Provides path for spice
Rin2 out1 gnd 325Meg      * Provides path for spice

*****
*U Element and termination
*****
U2 out2 gnd out3 gnd UT-47 l=30mm      *micro coax

```

Rout2 out3 gnd 50

*assume termination to ideal coax

*50GHz Low pass filter at end of coax

R1 out3 out4 1000

C1 out4 gnd20fF

*Materials FR4 at 1Ghz

.MATERIAL diel_fr4 DIELECTRIC ER=4.3 LOSSTANGENT=0.015

.MATERIAL diel_epoxy DIELECTRIC ER=4 LOSSTANGENT=0.015

.MATERIAL copper METAL CONDUCTIVITY=59.61meg

* Coax Shapes

.SHAPE whisker CIRCLE radius="whs_rad"

*whisker radius

.SHAPE micro_coax CIRCLE radius = "coax_inner_rad"

*coax inner conductor radius

*Uses the default AIR

*background

.LAYERSTACK stack_1 LAYER=(PEC, 1um) + LAYER=(air,2.5mm) +

LAYER=(diel_epoxy,1mm)

*Option settings

.FSOPTIONS opt1 PRINTDATA=YES ACCURACY=HIGH

*Two different conductor shapes

*Air coax

.MODEL whisker W MODELTYPE=FieldSolver,

+ LAYERSTACK=stack_1, FSOPTIONS=opt1,

+ RLGCFILE=coupled.rlgc

+ CONDUCTOR=(SHAPE=whisker,ORIGIN=

+ (2.5mm, 5mm), MATERIAL=copper)

+ CONDUCTOR=(SHAPE=micro_coax,

+ ORIGIN=("layer_pos", 5mm), MATERIAL=copper)

*layer_pos is specified C to C plus

2.5mm

*Model

*UT-47-M17 Micro coax

.MODEL UT-47 u LEVEL=3 plev=2 elev=1 wlump=30 maxl=300

```
+ RA=144um RB=470um RD=597um RHO=17n RHOB=17n KD=2.1
```

```
.MODEL air_coax u LEVEL=3 plev=2 elev=1
```

```
+ RA="whs_rad" RB=2.5mm RHO=52.9n RHOB=17n KD=1
```

```
*****
```

```
*Analysis, outputs and end
```

```
*****
```

```
.TRAN 1p 1.023n *use for tran
```

```
*.tf v(out2) V(1) *use for tran
```

```
*.AC Dec 1000 4GHz 40GHz *use for AC
```

```
*.PROBE v(out4) V(out3) v(in1) V(1) V(w_in) i(Rin1) i(Rw) *probe V(w_in) whisker input  
impedance
```

```
.OPTION INGOLD=2
```

```
.OPTION PROBE POST
```

```
.PROBE tran PAR('v(1)*1') PAR('v(out3)*1') PAR('v(out4)*1') *use for AC
```

```
*prints in exponential format
```

```
.PRINT PAR('v(1)*1') PAR('v(2)*1') PAR('v(out4)*1') *use for AC
```

```
.END
```

Appendix E – Matlab, Probe Hand Calculations

```
%Michael Jacob
%5.23.08
%Probe hand calculations
%lengths in meters or mm converted to meters

close all, clear all, clc; %matlab housekeeping

%% constants
c      = 3e8;           %light speed m/s
Eo     = 8.85e-12;      %permittivity of free space F/m
Uo     = pi*4e-7;       %permeability of free space H/m
ZL     = 50;            %termination impedance
freq   = 1e9;           %1GHz for determining electrical length
whis_len = 2.7e-3;      %2.7mm
whis_rad = 0.008e-3;    %0.008mm
whis_shld_rad = 20e-3;  %20mm
spacing = 0.37e-3       %whisker-tube spacing
overlap = 0.7e-3        %whisker-tube overlap that creates the
capacitor
Er      = 2.02;         %dielectric constant of Teflon
mc_wire_rad = 0.1435e-3; %radius of micro coax wire
mc_shld_rad = 0.47e-3;  %radius of shield
mc_len   = 30e-3;       %length of micro coax
tube_rad = 0.3e-3;      %tube that surrounds coax wire

%% Acquire the Impedance waveform in the test file generated by ADS
% Using this style ignores the ADS header
fid = fopen('C:\Documents\ADS\probe_hand_calc_prj\data\matlab_z.slp',
'r');
[s_matrix] = textscan(fid, '%f %f %f', 300, 'headerlines', 5);
fclose(fid);

% create a ninety X 1 column array from the ninety X 3 array
x      = s_matrix{1};    % get the first column data (frequency)
ads_Z   = s_matrix{2};    % get the second column data (real)
ads_angle = s_matrix{3};  % get the third column data (angle)
f       = x';            %rotate frequency matrix 90 degrees
%% microcoax calculations
mc_C    = 2*pi*Eo*Er/log(mc_shld_rad/mc_wire_rad); %per unit length
mc_L    = Uo/(2*pi)*log(mc_shld_rad/mc_wire_rad); %per unit length
mc_Zo   = sqrt(mc_L/mc_C) %50 ohm coax
vp      = c/sqrt(Er);
mc_Beta = 2*pi.*f./vp;
mc_elec_len = 360*mc_len*freq/vp
Z_last  = mc_Zo.*(ZL+j.*mc_Zo.*tan(mc_Beta.*mc_len))./(mc_Zo +
j.*ZL.*tan(mc_Beta.*mc_len));

%%capacitor calculation
separation = spacing-tube_rad-whis_rad
C          = 2*pi*Eo/acosh(2*separation/(2*whis_rad))*overlap %whisker
to plane approximation
XC         = 1./(j*2*pi*C.*f); %capacitive reactance
Z_mid      = XC+Z_last;

%% air coax calculations
whis_C    = 2*pi*Eo/log(whis_shld_rad/whis_rad); %per unit length
whis_L    = Uo/(2*pi)*log(whis_shld_rad/whis_rad); %per unit length
whis_Zo   = sqrt(whis_L/whis_C)
```

```

whis_Beta      = 2*pi.*f./c;
whis_elec_len  = 360*whis_len*freq/c
Zin            = whis_Zo.*(Z_mid+j.*whis_Zo.*tan(whis_Beta.*whis_len))./(whis_Zo
+ j.*Z_mid.*tan(whis_Beta.*whis_len));

%% approximate transfer function calculation
Hs            =(ZL./(ZL+Zin));
%% Plots
subplot (2,1,1);                % plot the impedance
loglog      (x/1e9,ads_Z, 'bo', 'MarkerSize',7); % ads calculation
grid
hold on;
loglog      (f/1e9, abs(Zin),'r','LineWidth',2); % matlab calculation
hold off;
title      ('Probe Input Impedance vs Frequency'); %detail the plot
xlabel      ('Frequency (GHz)');
ylabel      ('Impedance (Ohms)');
legend      ('ADS','Matlab');
subplot (2,1,2);                % plot the approx transfer function

semilogx      (f/1e9, 20*log10(abs(Hs)),'r','LineWidth',2); % matlab
calculation
grid
hold off;
title      ('Probe Approx. Transfer Function vs Frequency'); %detail the
plot
xlabel      ('Frequency (GHz)');
ylabel      ('H(s) (dB)');
legend      ('Matlab');

```

Appendix F – Matlab, HSpice to FFT

```

%%%%%%%%%%%%%%%%%%%%%%%%%%%%%%%%%%%%%%%%%%%%%%%%%%%%%%%%%%%%%%%%%%%%%%%%
%Author:    Michael Jacob
%Date:      8.14.07
%Revision:  8.21.07  8.22.07 Uses updated spice files that have
%input resistance as part of the DUT.
%This program loads HSpice simulation from a text file into the
workspace.
%A frequency domain transfer function is determined from a square wave
%input and the resulting system output using both direct non filtered
%output and 50GHz RC filter output
%%%%%%%%%%%%%%%%%%%%%%%%%%%%%%%%%%%%%%%%%%%%%%%%%%%%%%%%%%%%%%%%%%%%%%%%
close all;           %Matlab housekeeping
clear all;
clc;

%%%%%%%%%%%%%%%%%%%%%%%%%%%%%%%%%%%%%%%%%%%%%%%%%%%%%%%%%%%%%%%%%%%%%%%%
%Open HSpice .lis file, extract the data into a Matlab column matrix.
%Reshape the column matrix into a 4 row matrix
%and split into respective 1X matrices
%%%%%%%%%%%%%%%%%%%%%%%%%%%%%%%%%%%%%%%%%%%%%%%%%%%%%%%%%%%%%%%%%%%%%%%%
Fid = fopen('C:\Documents\Michael\'s
Classes\Probe\HSpice\whisker_coupler_coax_filter_simple_rev1.lis');
while 1
    tline = fgetl(fid);
    if ~ischar(tline), break, end
    if tline ==('x')
        tline = fgetl(fid);
header
    tline = fgetl(fid);
    tline = fgetl(fid);
    %read string data into column matrix until it reaches non
numeric
    SpiceData= fscanf(fid,'%g');
    len= length (SpiceData);
column matrix
    SpiceData=reshape(SpiceData,[4 len/4]);%reshape into 4 row
matrix
    end
end
fclose(fid);

time =      SpiceData(1,:);
clk_input = SpiceData(2,:);
input =     SpiceData(3,:);
output =    SpiceData(4,:);

%time matrix 0 to 1023ps
%input signal
%probe input signal
%LP 50GHz filtered output

%%%%%%%%%%%%%%%%%%%%%%%%%%%%%%%%%%%%%%%%%%%%%%%%%%%%%%%%%%%%%%%%%%%%%%%%
%figure 1
%plot HSpice pulse
%plot simulated transistor output
%plot probe output
%%%%%%%%%%%%%%%%%%%%%%%%%%%%%%%%%%%%%%%%%%%%%%%%%%%%%%%%%%%%%%%%%%%%%%%%
plot (time,clk_input,'y','LineWidth',2);
hold on
plot (time,input)
plot (time,100*output,'g')
%HS spice pulse
%Probe input
%Probe output X 100

```

```

legend ('DUT input vs time', 'Probe input vs time', 'Probe output X100 vs
time');
xlabel ('time (s)'),ylabel ('volts')
hold off
grid on;
%%%%%%%%%%%%%%%%%%%%%%%%%%%%%%%%%%%%%%%%%%%%%%%%%%%%%%%%%%%%%%%%%%%%%%%%
%Change the input and output signals into the frequency domain and
%deconvolve H(s) transfer function. Convert H(s) to h(t). Randomly
%choose 1024 points
%%%%%%%%%%%%%%%%%%%%%%%%%%%%%%%%%%%%%%%%%%%%%%%%%%%%%%%%%%%%%%%%%%%%%%%%
%Change to freq
X = fft(input,1024);
Y2 = fft(output,1024);
H2 = Y2./X; %filtered H(s)
%change transfer function back to time
h2 = ifft(H2, 1024); %filtered h(t)

%%%%%%%%%%%%%%%%%%%%%%%%%%%%%%%%%%%%%%%%%%%%%%%%%%%%%%%%%%%%%%%%%%%%%%%%
%View the time domain transfer function from probe input to filtered
output
%%%%%%%%%%%%%%%%%%%%%%%%%%%%%%%%%%%%%%%%%%%%%%%%%%%%%%%%%%%%%%%%%%%%%%%%
figure %2 %figure 2
plot (time,h2) %Impuse function
legend ('time domain transfer function vs time');
axis tight
grid on;
%%%%%%%%%%%%%%%%%%%%%%%%%%%%%%%%%%%%%%%%%%%%%%%%%%%%%%%%%%%%%%%%%%%%%%%%
%division of Y(s)/H(s)=X(s) which is the frequency representation of the
%original signal. An inverse Fourier transform derives x(t) (the
original
%signal)
%%%%%%%%%%%%%%%%%%%%%%%%%%%%%%%%%%%%%%%%%%%%%%%%%%%%%%%%%%%%%%%%%%%%%%%%
X_reconst2=Y2./H2;
x_reconst2= ifft(X_reconst2,1024);
figure %3 %figure 3
plot (time, x_reconst2,'y','LineWidth',2); %reconstructed input
hold on;
plot(time,input,'b--') %input signal
legend ('reconstructed input vs time by means of Fourier
transforms','Probe input vs time');
xlabel ('time (s)'),ylabel ('volts')
hold off;
grid on
%%%%%%%%%%%%%%%%%%%%%%%%%%%%%%%%%%%%%%%%%%%%%%%%%%%%%%%%%%%%%%%%%%%%%%%%
%Now test with an filtered input arbitrary waveform
%Open HSpice .lis file, extract the data into a Matlab column matrix.
%Reshape the column matrix into a 4 row matrix
%and split into respective 1X matrices
%%%%%%%%%%%%%%%%%%%%%%%%%%%%%%%%%%%%%%%%%%%%%%%%%%%%%%%%%%%%%%%%%%%%%%%%
fid=fopen('C:\Documents\Michael\'s
Classes\Probe\HSpice\whisker_coupler_coax_filter_simple_PWL_rev1.lis');
while 1
    tline = fgetl(fid); %read file line by line
    if ~ischar(tline), break, end %go until EOF
    if tline ==('x') %Look for beginning of data
        tline = fgetl(fid); %ignore the 3 line data
header
    tline = fgetl(fid);
    tline = fgetl(fid);

```



```

                                %read string data into column matrix until it reaches non
numeric
                                SpiceData_1= fscanf(fid,'%g');
                                len= length (SpiceData_1);           % the length of the column
matrix
                                SpiceData_1=reshape(SpiceData_1,[4 len/4]);   %reshape into 4
row matrix
                                end
end
fclose(fid);
%%%%%%%%%%%%%%%%%%%%%%%%%%%%%%%%%%%%%%%%%%%%%%%%%%%%%%%%%%%%%%%%%%%%%%%%
%plot HSpice pulse
%plot simulated transistor output
%plot probe output
%%%%%%%%%%%%%%%%%%%%%%%%%%%%%%%%%%%%%%%%%%%%%%%%%%%%%%%%%%%%%%%%%%%%%%%%
figure %4                                %figure 4
plot (time,SpiceData_1(2,:), 'y', 'LineWidth',2); %Hspice PWL pulse
hold on
plot (time,(SpiceData_1(3,:)))            %Probe input
plot (time,(100*SpiceData_1(4,:)), 'g')    %Probe output X 100
legend ('DUT input vs time', 'Probe input vs time', 'Probe output X100 vs
time');
xlabel ('time (s)'),ylabel ('volts')
hold off
grid on;

Y4 =  fft(SpiceData_1(4,:),1024);          %filtered sample
X_reconst4 = Y4./H2;
x_reconst4 = ifft(X_reconst4,1024);
figure %5                                %figure 5
plot (time, x_reconst4, 'y', 'LineWidth',2); %reconstructed input
hold on;
plot(time,SpiceData_1(3,:), 'b--')        %probe input
legend ('reconstructed input vs time by means of Fourier
transforms', 'Probe input vs time');
xlabel ('time (s)'),ylabel ('volts')
grid on;

```